THE STRUCTURAL EVOLUTION OF THE BULL CREEK AREA, SOUTHERN ADELAIDE FOLD BELT, SOUTH AUSTRALIA; THROUGH THE INTEGRATION OF GEOLOGICAL MAPPING AND GEOPHYSICAL INTERPRETATION.

Peta J. Saunders, B.Sc.

This thesis is submitted as partial fulfilment of the requirements
for the Honours Degree of Bachelor of Science

November 1993

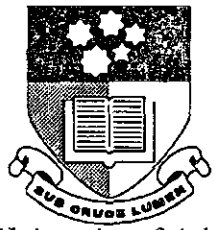

The University of Adelaide
The Department of Geology and Geophysics

Australian National Grid Reference
Milang (SI 54) 6627-II 1:50 000 Sheet

Supervisors: P R James, S Rajagopalan

Green pastures of the Bull Creek area with the Kuitpo Forest in the distance.

ABSTRACT

Integration of a high resolution aeromagnetic survey with detailed structural field data has been achieved in the Bull Creek area of the southern Adelaide Fold Belt, resulting in a comprehensive proposed model for the structural evolution of this area. Aeromagnetic data has placed constraints upon structures mapped at the surface and has also revealed information concerning the nature of structures at depth. The successful interpretation of data is due to the good lithomagnetic marker horizons within the area. These horizons include the magnetic Barossa Complex basement and lithomagnetic units of the Adelaidean Supergroup and Kanmantoo Group metsediments. The Brachina Formation, an important magnetic marker horizon of the Adelaidean Supergroup, lies at depth (due to thrust related tear-faulting) beneath a magnetic cover of Backstairs Passage Formation of the Kanmantoo Group sediments.

Geophysical images and contour maps reveal the location and intensity of important magnetic and radiometric anomalies which constrain the interpretation of mapped structures. Modelling of individual magnetic profiles places constraints on the depth to the top, the width, dip and susceptibility of magnetic bodies. Vertical gradient filtering enhances the edges of two dimensional sources and Automated Gains Control filtering amplifies the effects of small anomalies.

A model suggesting multiple sequential thrusting has been devised for the Bull Creek area. This model incorporates a basal décollement located within the basement (4-5 km beneath the present erosion level) which has transported a sliver of basement complex to the surface where it forms a hangingwall anticline. An upper detachment has formed near the basement - cover contact within the basal unit of the Adelaidean sequence. High angle listric thrusts of an imbricate fan (or sigmoidal faults of a duplex system?) stem from this detachment fault.

TABLE OF CONTENTS

ABBREVIATIONS AND UNITS

AGC	Automatic Gain Control
BCSZ	Blackfellows Creek Shear Zone
BCT	Bull Creek Thrust
CPS	Counts Per Second
CRAE	Con-zinc Rio Tinto Australia Exploration Pty Ltd
MCFTS	McHarg Creek Folded Thrust Sheet
MMR	Mount Magnificent Re-entrant
NRM	Natural Remanent Magnetisation
SADME	South Australian Department of Mines and Energy
SRIF	Still Range Imbricate Fan
SSCT	Sheep Station Creek Thrust
TMI	Total Magnetic Intensity
VG	Vertical Gradient

Magnetic susceptibility is measured in S.I. units

Magnetic intensity is measured in nanoTeslas (**nT**)

Radiometric intensity is measured in counts per second (**CPS**)

LIST OF FIGURES

LIST OF PLATES

1. INTRODUCTION

1.1 Introduction

Continental orogenic belts of complex structural geometry and evolution, may hold key information concerning the tectonic processes which have operated to produce such belts. Significant outcrops however are often of limited extent. In small areas it may be possible for geological and structural data to be obtained from every outcrop. However if there is limited outcrop, the definition of stratigraphic boundaries is impeded and the continuity of structures is difficult to predict, especially in structurally complex areas. The interpretation of geological structures at depth is based on the extrapolation of outcrop observations and is not constrained, unless drill or seismic data is available.

Geophysical airborne surveys commonly record both aeromagnetic and radiometric information and improve sampling by providing information at regular intervals. Geological mapping which is governed by outcrop distribution, cannot match this coverage. Geophysical information obtained from magnetic surveys reflects the distribution of magnetic minerals within various rock types (Grant, 1985). Lithomagnetic units producing a characteristic anomaly are of great importance as magnetic marker horizons which may be traced over large distances. Radiometric information is a reliable indicator of lithology and successfully records subtle differences in the geochemical composition of rock types (Telford, 1990).

Subsurface information to depths of about 20km at the Curie isotherm is recorded by aeromagnetic surveys (Telford, 1990). The signal received is a combination of magnetic contributors from the surface and underlying units to great depths, and is unaffected by outcrop distribution. The success of aeromagnetic surveys relies on the sufficient variation in the magnetic susceptibility of rock units. In comparison to aeromagnetic information, the signal received from a radiometric survey is the result of signal contributions from only the top 50cm of outcrop, providing valuable constraints on lithological boundaries at the surface.

Geophysical data of a high quality is now readily available. The collection of digital data and the evolution of new computer software packages have made the display and subsequent interpretation much easier than in the past (Rajagopalan and Boyd, 1989). With the use of geophysical data the reinterpretation of previously mapped areas may be greatly improved. Whiting (1986) successfully achieved a more complete interpretation of the poorly exposed Arunta Inlier, NT, through the integration of aeromagnetic and geological data. Magnetic data not only revealed structures which did not outcrop, but further constrained and refined

structures which had been mapped. The advent of new integrated geophysical and structural computer modelling programs (Valenta et al, 1992) leads the way for geophysical data to be readily integrated with mapped geology.

Geological and structural data collected in the field combines with geophysical data to produce a complementary data set and results in a more informed geological interpretation. This can only lead to a better understanding of the evolution of geological structures and may elude to the nature of the tectonic processes involved in the formation of orogenic belts. The current study uses an integrated survey of field structural mapping and detailed, high resolution geophysical data to assist in understanding the geology and structure of a small complex area in the southern Adelaide Fold Belt of South Australia.

1.2 Regional Geology and Geophysics

The southern Adelaide Fold Belt extends for 200km from the Mt. Lofty Ranges through the Fleurieu Peninsula to Kangaroo Island in the south (Figure 1). The major structural trend varies from north-south in the Mt. Lofty Ranges to east-west on Kangaroo Island and this structural trend curves around the Fleurieu Arc (Mancktelow, 1990). The Fold Belt consists of a series of Lower to Middle Proterozoic basement inliers which form the core of a major anticlinorium (Clarke and Powell, 1989). On either side of these inliers are Late Proterozoic Adelaide Supergroup sediments and Cambrian Normanville and Kanmantoo Group metasediments (Figure 1), which were deposited in an extensional basin formed due to cyclical stretching of the lithosphere (Jenkins, 1990)

A major orogenic event, the Delamerian orogeny is proposed to have occurred in the Late Cambrian to Early Ordovician (Parkin, 1969). This led to the compression and subsequent fold and thrust deformation of sediments of the Adelaide Geosyncline and the Kanmantoo basin. Magnetic marker horizons within the fold belt have previously been interpreted (Rajagopalan, 1989) provide extra information which may be used to unravel Delamerian associated deformation. These horizons include the basement, and lithomagnetic units within both the Adelaide Supergroup and Kanmantoo Group.

1.3 Previous Investigations and Present Controversy

Traditional interpretations accounting for the formation of the southern Adelaide Fold Belt are being reviewed by researchers at The University of Adelaide. Early regional mapping (Offler and Fleming, 1968 and Mancktelow, 1979b) suggested that compressional deformation has induced large scale folds which are the dominant structures within the fold belt. Recent workers (Jenkins, 1986,1990, Sandiford and Jenkins, 1991, Clarke and Powell, 1989, Steinhardt, 1991) have suggested that deformation within the fold belt has occurred as the result of a thin skinned tectonic regime. It has been suggested that the primary structures dominating

the area are the major thrust faults (and their associated folds) of a foreland basin province (Jenkins 1990). Through recent detailed field investigations (Johnson, 1991, Rogers, 1991 and Menpes, 1992) it appears that more evidence is lent to the recently suggested thrust dominated regime.

1.4 Location and Physiography of the Bull Creek Area

The Bull Creek area, lies approximately 60km south of Adelaide in the central Fleurieu Peninsula. It is situated within the southern Adelaide Fold Belt in the Fleurieu Arc region (Figure 1). Topographic relief varies from 100m in creeks to 420m above mean sea level at North of Mount Magnificent. Bull Creek forms part of South Australia's dairy farming district and is characterised by farm pastures and steep grassy hills. Outcrop is sparse in this region due to farm use and large pine forests (see frontispiece), it is therefore restricted to road cuttings, creeks and to a few steep outcropping escarpments.

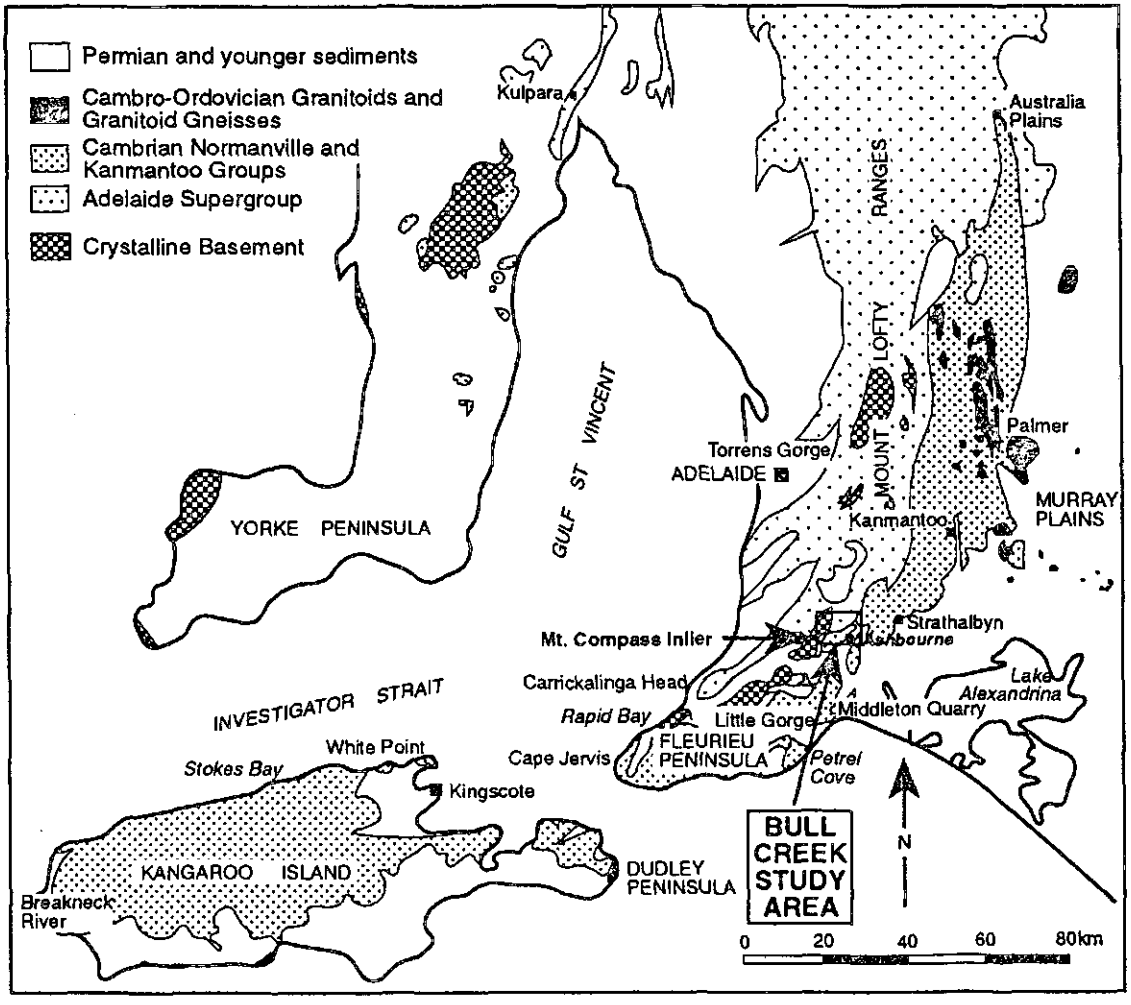

Figure 1 Location of the Bull Creek area within the southern Adelaide Fold Belt (after Mancktelow, 1990). The shaded rock units show the arcuate trend of the Fleurieu arc.

1.5 Aims and Methods of Investigation

From previous mapping (Wymond, 1950, Heaslip, 1972 and Mancktelow, 1979b) of the study area it has been shown that the Bull Creek area presents the following geological problems.

- Stratigraphic units in the area appear to be repeated.
- Adelaide Supergroup sediments are thicker to the north of the study area and appear to terminate in the south of the area.
- Where termination of the Adelaidean sediments occurs, substantial thickening of the Kanmantoo Group metasediments is observed.

By addressing these problems this research project is aimed at providing an improved interpretation for the evolution of geological structures in this region of the southern Adelaide Fold Belt. A working method for integrating structural field data and geophysical data was established and may benefit further studies in other areas.

Outcrop mapping of an area approximately 50km^2 was carried out on a 1:10 000 scale using composite aerial photographs and topographic maps as a base. Structural data collected included bedding, cleavage and lineations, which are presented on 1:25 000 scale maps. Oriented samples were collected and thin sectioned to reveal microstructural detail and for mineralogical analyses to be carried out.

Interpretation of aeromagnetic and radiometric data (obtained from CRAE) was completed using 1:25 000 scale maps and are presented at a 1:50 000 scale. These maps were produced using various filters and methods of display to enhance the geophysical signal from different rock units. To provide constraints on aeromagnetic interpretation, susceptibility measurements were taken in the field at all outcrop stations. Magnetic anomalies in key areas were modelled to constrain width estimates, depth to the top of magnetic units, and to provide estimates of the dip of lithomagnetic units.

2. STRATIGRAPHY

2.1 Introduction

Stratigraphic nomenclature was originally assigned in this region by Mawson (1939) and Wymond (1950). The most recent map sheet (Milang 1:63 360 SADME 1963) covers the study area, but its stratigraphic nomenclature is now obsolete. The stratigraphy used in this study is based on the extrapolation of stratigraphic units of the Echunga and Noarlunga (1:50 000 SADME 1982) map sheets which lie directly north of the study area. Due to the limited outcrop the precise nature of contacts between rock units was not able to be discerned in detail. It should also be noted that some stratigraphic formations may be present subsurface, but have not been mapped because they do not outcrop within the study area. It was important to this study that the stratigraphy was adequately recognised, as repetition of this stratigraphy forms the basis of some structural interpretations.

Lithology of outcrops was described and compared with the previously defined stratigraphy to confirm the names of the formations which have been applied in the study area (Figure 3.2: Map 1). Stratigraphy was based on lithological and sedimentological interpretation. Magnetic data was used to assign lithomagnetic units (Figure 2), which are based on the distribution of magnetic anomalies and magnetic susceptibility readings.

2.2 Barossa Complex

Throughout the southern Adelaide Fold Belt the multiply deformed Barossa Complex forms the basement to the overlying Adelaidean cover sequence. It is exposed as a series of inliers which were described as anticlinal cores (Parkin, 1969) that have been exposed through stripping of the overlying sedimentary cover . The western edge of the Bull Creek study area is comprised of the northern part of the Mt. Compass Inlier (Figure 1). Due to the Kuitpo Forest and the Kyeema Conservation Park in this area, outcrop is restricted to road cuttings and some creeks.

The basement varies compositionally between quartz-garnet phyllonites, and biotite schists. Within the quartz-garnet phyllonite there is a prominent compositional layering. This consists of bands of sheared quartz (which are white to blue) and pale pink garnet clasts which alternate with bands of muscovite and fine grained sericite (which gives the rock an orange sheen). An oyster shell texture is observed on schistosity planes defined by micaceous minerals covering elongate quartz clasts. The presence of sericite, which has resulted from the recrystallisation of K-Feldspars, and altered garnets (Plate 1) indicate a retrogressive phase of metamorphism has occurred. The biotite schists mineralogically consist of biotite, quartz, chlorite, magnetite and

Stratigraphy

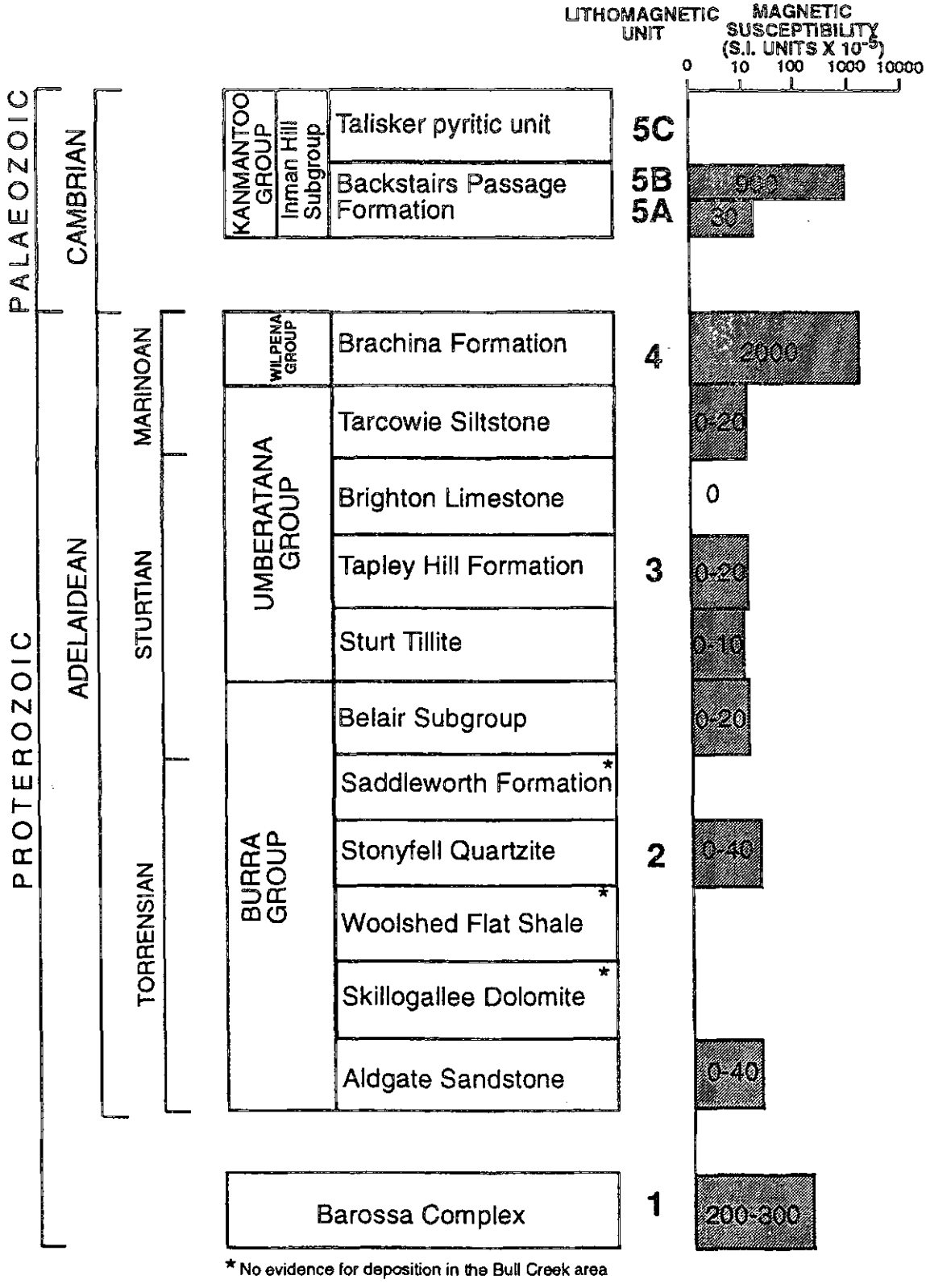

Figure 2 Stratigraphy of the Bull Creek area (adapted from SADME Noarlunga and Echunga 1:50 000 map sheets,1982). Lithomagnetic units occur within stratigraphic units but do not necessarily comprise the whole stratigraphic unit. Units have been assigned a number (1-5C), and are discussed in detail in Chapter 4. Magnetic susceptibilities presented were obtained from outcrop. These values are the averages of 10 to 50 readings, which were limited by outcrop size.

rare garnet and amphiboles. Magnetite is responsible for the high magnetic amplitude of the basement. Greater amounts of magnetite occur in the biotite schists than the phyllonitic units. This magnetite variation may be responsible for the irregular distribution of magnetic anomalies (discussed in Chapter 4) within the basement. The basement is denoted as lithomagnetic unit 1.

2.2 Adelaide Supergroup

2.2.1 Burra Group

a) Aldgate Sandstone

Overlying the basement complex is the basal conglomerate of the Aldgate Sandstone which is found to outcrop in only a few areas in the study region. It has been estimated through field mapping to be 250 metres thick and varies in composition along strike. In the north, large elongate quartzite and quartz clasts vary in size from 2-400mm and are surrounded by a pelitic matrix which anastamoses around these clasts (Plate 2). To the south the conglomerate is a soft friable cream coloured sandstone with heavy mineral bands , that supports elongate quartz and quartzite clasts (2-50mm). This southern unit is divided into distinct bands (about 50cm thick) which consist of a coarse sandstone without clasts and a coarse sandstone containing clasts (Plate 3). The quartz clasts are blue which suggests an igneous source. This is supported by the conglomerates' proximity to a presumed deformed meta-igneous basement.

The Aldgate Sandstone has been mylonitised in the south along the Blackfellows Creek Shear Zone (BCSZ) (Figure 3.2: Map 1). This mylonite is characterised by pink and white bands which consist of recrystallised feldspars and quartz (which occur as ribbons), with some discontinuous bands of ilmenite which are remnants of heavy mineral banding. Remnant quartz and feldspar clasts in the outer areas of the shear zone occur within a recrystallised quartz and feldspar matrix. In these areas much of the feldspar has been kaolinised producing a soft and friable rock.

b) The Skillogalee dolomite and Woolshed Flat shale are absent in outcrop in the study area, but may be present subsurface.

c) Stonyfell Quartzite

The Stonyfell Quartzite which is 400m thick in type section (Preiss 1987), appears as an apparently thickened sequence of approximately 2 kilometres overlying the Aldgate Sandstone. This formation terminates in the south against the Sheep Station Creek Thrust (SSCT) (see Figure 3.2: Map 1). Stonyfell Quartzite also outcrops as a 350 metre thick band overlying younger stratigraphic units which thins to the south where it is terminated by the SSCT. This unit consists of white quartzite and consolidated sandstones which have shale interbeds. The quartzite is composed almost entirely of well sorted and well rounded medium sized quartz

grains and contains some concentrations of heavy mineral bands. Sericite is commonly present as an orange sheen along fracture surfaces. The maturity of this unit is consistent with Preiss' (1987) suggestion that it has a distal source. Cross beds within the quartzite, defined by heavy mineral bands, indicate an easterly younging direction. This implies a right way up for both layers of this formation in the study area. Stonyfell Quartzite contains small magnetic anomalies with low susceptibilities which constitute lithomagnetic Unit 2.

d) The Saddleworth Formation is absent in outcrop in this study area, but its presence subsurface cannot be ruled out.

e) Belair subgroup

In the study area the Belair subgroup occurs as two bands which are both approximately 500 metres thick. The Belair subgroup is distinguished by feldspathic quartzites, sandstones and minor siltstones which are kaolinised in parts. The quartzites are pale pink to grey Mineralogically the sandstones consist of medium size grains of quartz and feldspar, and the siltstones comprise of fine grained mudstone

2.2.2 Umberatana Group

a) Sturt Tillite

The Sturt Tillite occurs as a massive dark grey unit which shows no distinct bedding. The Sturt Tillite is repeated and occurs as two distinct bands which are separated by other stratigraphic units. The units are approximately 40-50 metres thick and trend roughly north-south, but are both terminated to the south by the Sheep Station Creek Thrust (Figure 3.2: Map 1). Clasts within the Sturt Tillite range in size from 2-100mm. These are poorly sorted and range from angular to well rounded. Quartz and quartzite clasts are abundant, with minor carbonate and gneissic clasts. The matrix supporting the clasts comprises dark grey, fine grained micas and clay minerals.

b) Tapley Hill Formation

The Tapley Hill Formation is extensively deposited throughout the Adelaide Geosyncline (Preiss 1987). In the study area the Tapley Hill Formation is characteristically dark blue-grey and varies from calcareous shales to well laminated slates. The laminations occur as couplets, which are repeated on approximately 2-5mm scale and are made up of dark pelitic and pale psammitic layers (Plate 4). In slaty units ripple marks are well preserved and indicate an easterly younging direction (Figure 3.3: Map 2). The Tapley Hill contains the lithomagnetic marker horizon, Unit 3 which has low susceptibility.

c) Brighton Limestone

The Brighton Limestone is not present as a discrete stratigraphic horizon but occurs as bands within and near the top of the Tapley Hill Formation. In the study area the Brighton Limestone has been mapped as two distinct 1-5m thick coarse grey marble units which are almost completely recrystallised (Plate 5) and appear buff coloured in outcrop. These units are especially prominent in the hinge of the major folds in the area (see Figure 3.2: Map 1).

d) Tarcowie Siltstone

The Tarcowie Siltstone varies between a grey laminated siltstone at the top, with a massive fine grained buff coloured sandstone to pale brown grey tillite at the base of the sequence. The unit is dolomitic in some areas and displays heavy mineral laminations in sandstone horizons. Within the study area it appears to thin and is terminated to the south by the Bull Creek Thrust (Figure 3.2: Map 1).

2.2.3 Wilpena Group

a) Brachina Formation

The Brachina Formation is a finely laminated siltstone, displaying a characteristic steel grey colour when fresh, and a rusty brown colour in weathered outcrop. The unit is phyllitic in some horizons and sandier in others. The Brachina Formation is rich in magnetite content and has a high magnetic susceptibility and a high positive magnetic anomaly. The Brachina Formation is an important lithomagnetic horizon and is denoted as Unit 4.

The basal Cambrian Normanville Group and Carrickalinga Head Formation are absent in the study area though they are present 1-2 km north.

2.3 Kanmantoo Group

2.3.1 Inman Hill Subgroup

a)Backstairs Passage Formation

The base of the Backstairs Passage Formation is marked by a medium grained, cream coloured sandstone with distinct heavy mineral laminations. The heavy mineral laminations define cross beds and indicate easterly younging (Figure 3.3: Map 2). Overlying units, of the same formation are homogeneous, massive, pale grey consolidated sandstones, within which are pink-grey arkosic units. The sandstones comprise of medium sized quartz and feldspar grains, with minor biotite and magnetite. The arkosic units are more feldspathic and contain magnetite bands. Both Units 5A and 5B are comprised of Backstairs Passage Formation.

b)Talisker Formation

The Talisker Formation occurs near the Adelaidean - Kanmantoo contact. It consists of a finely laminated, dark grey pyritic siltstone, which appears in weathered outcrop with yellow and

orange sulphur and iron staining on it. This unit is made up of fine grained quartz and biotite, with lenticular pyrite bands. It is proposed that the lithomagnetic Unit 5C lies within the Talisker Formation.

2.5 Implications for Structural Interpretation

The distinct repetition of the Belair subgroup, the Sturt Tillite and the Tapley Hill Formation is undoubted (Figure 3.2: Map 1). As the bedding in the area is uniformly steeply dipping to the east a homoclinal sequence has previously been interpreted (Wymond, 1950). However since stratigraphic repetition occurs this homoclinal sequence is invalid. Suggestions that repeated units are the limbs of isoclinal folds may account for repetition however, opposing younging directions would be expected on these limbs. Within these repeated units only easterly younging directions are recorded. A model which may account for stratigraphic repetition with younging directions oriented in the same direction, is one which adopts thrust faulting as the main mode of deformation. The unusual termination of Adelaidean sediments against the SSCT and the BCT, the apparent thickness (2km) of the Stonyfell Quartzite and the abrupt termination of the Brachina Formation in the south, present complex stratigraphical problems. By the assessment of geological structures and the application of thrust tectonics to this region these stratigraphic enigmas may be unravelled.

3. STRUCTURAL DOMAINS

3.1 Introduction

A thrust sheet is a volume of rock bound below by a thrust fault, which exhibits a distinct stratigraphy, state of strain or metamorphic grade (Boyer and Elliot, 1984). The study area has been divided into structural domains primarily on the basis of thrust sheet determination. These domains exhibit characteristic bedding, cleavage, fold styles and strain states, which are common within each sheet but vary between sheets.

The structure of the area is dominated by a series of north to northeast trending thrust faults (the Bull Creek Thrust (BCT), the Sheep Station Creek Thrust (SSCT), Thrusts 1, 2, 3 and 4 of the Still Range Imbricate Fan (SRIF) and the Kuitpo Thrust) which bound thrust sheets (Figure 3.1). These occur mostly subparallel to the dominant bedding in the area, which has an average trend of 020 and dips steeply east (Figure 3.2: Map 1). However some faults, eg. BCT, SSCT are distinctly discordant truncating a number of stratigraphic units. The thrust sheets have been named the McHarg Creek Folded Thrust Sheet, the Still Range Imbricate Fan and the Mt. Magnificent Re-entrant Sheet mentioned by Jenkins (1990), separated from the basement by the Blackfellows Creek Shear Zone. The nature and implications of the various structural features, bedding, cleavage, lineations, folds and faults (Figure 3.3: Map 2), are described for each of the allocated structural domains.

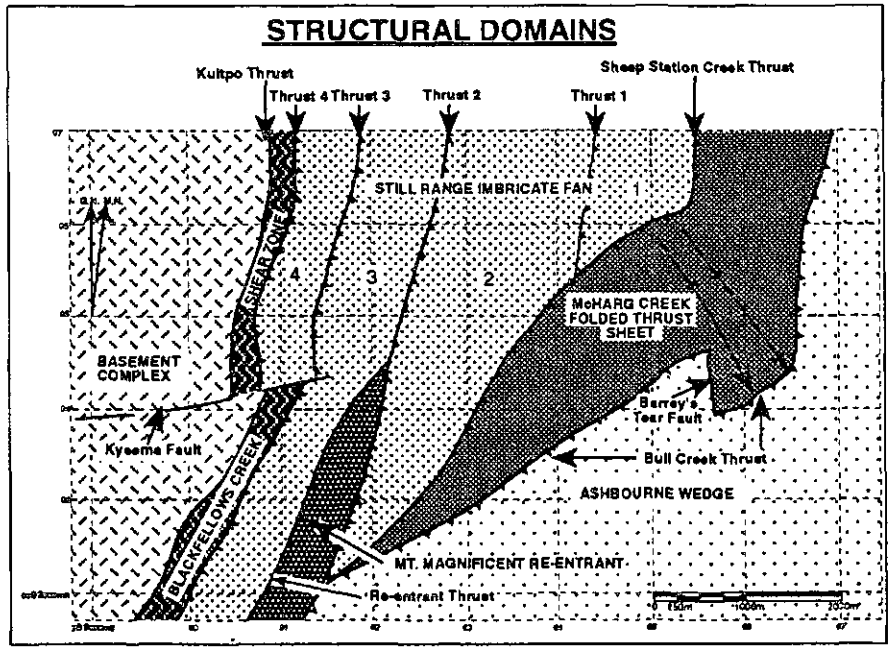

Figure 3.1 The Bull Creek area is divided into structural domains based on thrust sheet differentiation. Lithologies within thrust sheets are shown on Figure 3.2: Map 1.

3.2 Basement Complex

The basement was previously mapped (Heaslip, 1972) as an anticlinal inlier. However, only the eastern limb was mapped during this study. Inferences concerning the anticlinal nature of the basement are drawn from Heaslips mapping (1972). The basement is comprised of a thrust sheet which has been transported from a basal thrust (décollement) and folded to form a hangingwall anticline according to the nomenclature of Boyer and Elliot (1982) (see cross section, Figure 3.4). The basement inlier is offset by the Kyeema Fault, which has been inferred through the east-west displacement of the overlying basal conglomerate of the Aldgate Sandstone.

Within the basement the dominant fabric is a schistosity, which strikes north-south and dips 60° to the east. This fabric is associated with Delamerian deformation, as it is oriented in the same manner as the dominant cleavage in the overlying cover sequence. The basement contains elongate porphyroclasts of quartz indicating an elongation lineation that plunges 60° to the east. Micaceous minerals form a mineral lineation which is parallel to this elongation lineation. Lineations are taken to indicate movement direction and imply an east-west movement direction in the basement domain. The basement has been subjected to deformation prior to Delamerian deformation. This is evident in thin sections containing porphyroblasts with magnetite inclusion trails, which preserve an earlier fabric oblique to the Delamerian schistosity surrounding these porphyroblasts (Plate 6). Further evidence supporting this is the presence of high grade metamorphic minerals such as garnet and amphiboles. These do not conform with the suggested metamorphic grade for this area, derived from this study, and that of Offler and Fleming (1968) and Mancktelow (1979b) which indicate overlying cover sediments exhibit low grade chlorite-biotite grade metamorphism.

Basement-Adelaidean contact - SHEAR ZONE

The basement-Adelaidean contact is one of high strain and is defined by the Blackfellows Creek Shear Zone (BCSZ). Shearing occurs within the basal conglomerate of the Aldgate Sandstone, with strain varying from highly deformed pebble clasts, to mylonitisation and ultramylonitisation where almost total recrystallisation of minerals has occurred. Along the western contact strain is lower and results in deformation of pebble clasts in the Aldgate sandstone. Outcrop south of the Kyeema Fault exhibits bedding which is defined by heavy mineral laminations and lithological variation and dips steeply to the east. The dominant cleavage within this unit is oriented steeper to the east than the bedding (Plate 2). A schistose fabric exists in the conglomerate north of the Kyeema Fault. This is oriented north-south and dips steeply to the east. The orientation of this is similar to the cleavage found in the southern area. Lineations in the southern part of the BCSZ show the maximum elongation of clasts to

be 35°—>160°. However, clasts in the northern half of the BCSZ exhibit a differently oriented maximum elongation of 75°—>110°.

Lineations show conflicting orientations, however they are parallel to the direction of thrusting as described to the north and south of the Kyeema Fault. It is considered that the thrust propagation direction is parallel to elongation lineations which are perpendicular to the resulting thrust fault. This implies that the thrusts associated with the northern part of the Blackfellows Creek Shear Zone have propagated in a north south trending direction and the thrusts in the south have been transported in a NW-SE direction. Basement topography and possible ramps may be responsible for this variation in thrust transport direction.

The eastern part of the shear zone is comprised of mylonitised Aldgate sandstone, varying from a mylonite (Plate 7) on the edges of the shear zone, to an ultramylonite within the shear zone. Fault related rocks within the shear zone have been classified according to the nomenclature of Sibson (1977) and Wise et al (1984). Feldspar and some quartz porphyroclasts occur within the mylonite. These are defined as dominantly sigma type porphyroclasts using the nomenclature of Passchier and Simpson (1989). The identification of these porphyroclasts as sigma type makes their use as kinematic indicators valid, and implies a movement direction of top to the northwest. The ultramylonite is characterised by white ribbon quartz which defines a maximum elongation direction 30°–> 090°. The matrix is comprised of recrystallised microcline and plagioclase and remnant ilmenite.

3.3 Still Range Imbricate Fan

This domain comprises an imbricate fan consisting of four thrust sheets bound by thrust faults cutting the stratigraphic units up section (see Figure 3.4). The western two sheets (denoted 3 and 4) expose only Stonyfell Quartzite at the present erosional surface. Thrust sheet 4 is bound below by Thrust 4, which has developed along the eastern margin of the Blackfellows Creek Shear Zone. Sheet 3 is bound below by Thrust 3, this fault may account for the apparent thickening of the Stonyfell Quartzite. Thrust sheets 1 and 2 display a complete stratigraphic sequence, from the Stonyfell Quartzite to the Tapley Hill Formation (see Figure 3.2: Map 1). Thrust faulting is responsible for bringing sheets up from depth and placing older units in juxtaposition with younger units (eg. the Stonyfell Quartzite of Sheet 1 and the younger Tapley Hill Formation of Sheet 2). The sequence and mode of thrusting are described in detail in Chapter 5.

Bedding trends within the SRIF are consistent, averaging 60°80° towards 110°-120°. Bedding is easily detected in the Tapley Hill Formation (due to sedimentary laminations) and does not appear to vary between thrust sheets 1, 2, 3 and 4. It is more difficult to detect in the Belair

Subgroup and Stonyfell Quartzite as these are more massive units. Within the Sturt Tillite it is virtually absent and cleavage becomes the more dominant fabric.

Cleavage is poorly developed within quartzites and sandstones and exists as a penetrative/flaky cleavage subparallel to bedding, with average orientation of about 60° towards 100°. Crystal plastic deformation resulting in dynamic recrystallisation and subgrain formation, is the dominant deformation mechanism of the quartzites in the area. Within the Tapley Hill Formation in the vicinity of Thrust 1 a very well developed slaty cleavage has developed. This is oriented 75° towards 100° and is 30° steeper than bedding here (Plate 10). This cleavage is a slaty cleavage and is defined in the more pelitic laminations. Diffusive mass transfer is responsible for the solution cleavage that has developed in the Tapley Hill Formation (Plate 9) which lies very close to the top of a thrust sheet.

Lineations within the SRIF are present as mineral and elongation lineations. Mineral lineations occuring within the Tapley Hill Formation and elongation lineations occurring within the Stonyfell Quartzite (Plate 11), are oriented 60° towards 110°, supporting a SE-NW movement direction.

Thin section examination of the Sturt Tillite reveals pull apart clasts (Plate 8) in the vicinity of thrust faults (viz. the SSCT), which provide evidence for high strain in these areas. The Tapley Hill Formation also shows evidence for high strain near Thrust 1. Psammitic layers display elongation of quartz porphyroclasts and a very well developed solution cleavage.

The only folding evident in the SRIF is minor kink folding which occurs in the Stonyfell Quartzite. These kinks are asymmetric (Plate 12) and indicate a top to the NW movement direction. The folds plunge 10° towards 190° and have an axial plane which dips 30° towards 280°.

3.4 McHarg Creek Folded Thrust Sheet (MCFTS)

This sheet is bound at the base of the Tapley Hill Formation by the SSCT which is a NE-SW trending fault truncating Adelaidean sediments of the SRIF. The eastern boundary of the MCFTS is defined by the BCT, which truncates thrust sheet sediments at the south of the MCFTS, in a manner similar to the SSCT. Shearing of underlying Tarcowie tillites also occurs along the BCT.

The MCFTS is folded on a large scale, shown by a major anticline-syncline pair which are close, almost upright folds. Stereographic analysis (Figure 3.2: Map 1) has determined that these folds plunge 70° towards 125° and have a fold axial plane which is oriented 80° towards

035°. Folding has occurred during thrusting and has developed in the Tapley Hill Formation as it is a less competent unit.

Minor folds are confined in this domain to the calcareous units of the Tapley Hill Formation. Folds are asymmetric S folds which show variation in limb length. Folds also display limb thinning and hinge thickening and vary from gentle to open (Plate 13). These folds plunge shallowly (10°-35°) to the north (000°-030°). The asymmetric nature of these S shaped folds implies a top to the west sense of movement, which appears to conform to the west to north west tectonic transport direction previously suggested .

The Brachina Formation is characterised by 3 different types of folds: chevron style, kink style boxfolds and conjugate kink folds. In the vicinity of the major anticline are tight chevron style folds (plunging 80° towards 170° with fold axial planes 80° towards 080°) (Plate 14). These remain as chevron style but become more open away from the hinge of the major fold. Kink folds and conjugate kink folds (Plate 15) dominate the northern area of the Brachina Formation which is not affected by the major folds. Microscopic conjugate kink folds of the Brachina Formation mirror outcrop scale folds of this type in both morphology and orientation (Plate 16). Box folds occur between the two zones. These are typically kink style box folds (Plate 17) with conjugate fold axes. The dominant folds are characterised by fold axes 70° towards 040° and plunges of 70° towards 020°. The less dominant folds plunge 60° towards 200° and have fold axial plane oriented 60° towards 150°.

3.5 Kanmantoo Group Subdomains

Kanmantoo Group metasediments of the area are divided into two areas

a) The Ashbourne Wedge

b) The Mt. Magnificent Re-entrant.

a) The Ashbourne Wedge

This is bound at the base by the BCT which cuts across stratigraphy of Adelaidean sediments and may possibly fault out the lower Cambrian stratigraphy (eg. Normanville Group and Carrickalinga Head Formation) which may be present at depth. The Backstairs Passage Formation with heavy mineral bands is microfaulted and exhibits reverse sense thrusts (Plate 18) indicating top to the west movement. This is further evidence to suggest tectonic transport in this direction.

East of the Bull Creek Thrust zone the Kanmantoo Group (Backstairs Passage Formation) appears homogeneous and forms a homoclinal sequence (Wymond 1950), though upon closer investigation the folded nature of the rocks becomes more apparent. The folds (Plate 21)

exhibit steeply dipping fold axial planes (80° towards 090°) and parallel limbs which all dip steeply eastwards. These folds exhibit pronounced hinge thickening and limb thinning and have been classed as tight Class II similar folds which plunge 70° towards 010°.

b) The Mt. Magnificent Re-entrant

Jenkins (1990) recognised the re-entrant of Kanmantoo Group sediments near Ashbourne and suggested that it resulted from the amalgamation of thrust sheets in the vicinity. Outcrop is characterised by a well developed S_1 cleavage which is accompanied by exhibition of high strain. This high strain may be related to Thrust 2 and the Re-entrant Thrust.

3.6 Discussion

The strike of bedding varies between thrust sheets while the dip remains steep to the east in most cases. The SRIF exhibits strike of bedding 020, the MCFTS exhibits varying strikes as it is folded and the Ashbourne wedge exhibits north south striking bedding. Cleavage is shown to vary between thrust sheets and is very well developed in the vicinity of thrust faults. Areas of well developed cleavage and highly strained zones appear to correlate with thrust fault areas. However this correlation does not necessarily take into account that cleavage and strain may vary with lithology and not just proximity to fault zones. The orientation of major faults, lineations, porphyroclasts, asymmetric folds and microfaults indicate a dominant transport direction of thrust sheets. A major westerly tectonic transport direction is suggested for the northern half of the study region and a northwesterly tectonic transport direction for the southern section.

Figure 3.2

GEOLOGY OF THE BULL CREEK AREA, SOUTHERN ADELAIDE FOLD BELT

Map 1 Bedding

LOCALITY MAP

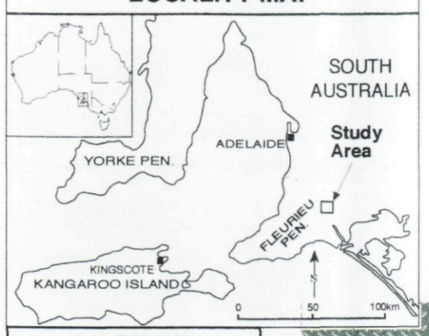

Regional Bedding

210 data Contoured 1 2 3.... times uniform

Major Fold within McHarg Creek Thrust Sheet

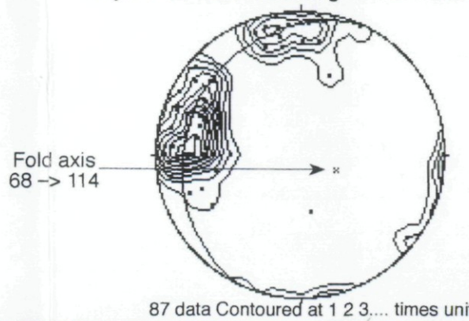

87 data Contoured at 1 2 3.... times uniform

LEGEND

- Bedding So (inclined) 70
- Bedding So (vertical)
- Lithological boundary
- Normal Fault
- Thrust Fault (inferred)
- Thrust Fault (mapped)
- Anticline
- Syncline
- Shear zone
- Roads
- Creeks

STRATIGRAPHIC COLUMN

- Talisker pyrite unit
- Backstairs Passage Fm
- Brachina Fm
- Tarcowie Siltstone
- Brighton Limestone
- Tapley Hill Fm
- Sturt Tillite
- Belair Subgroup
- Stonyfell Quartzite
- Aldgate Sandstone
- Barossa Complex Basement

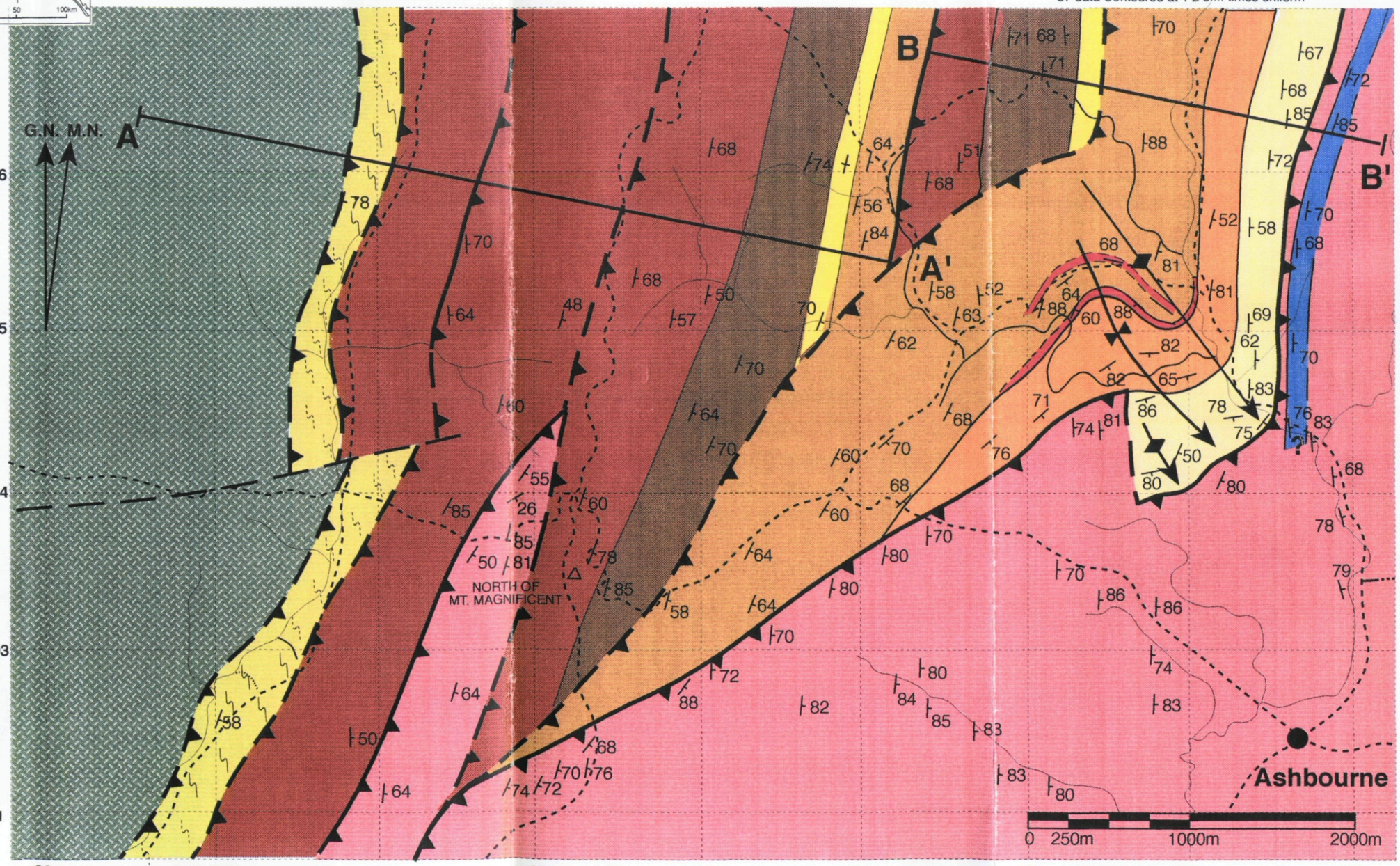

Peta Saunders 1993

Figure 3.3

GEOLOGY OF THE BULL CREEK AREA, SOUTHERN ADELAIDE FOLD BELT

Map 2 Cleavage Lineations

LOCALITY MAP

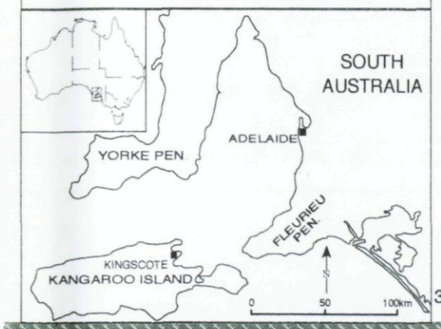

Regional Lineations

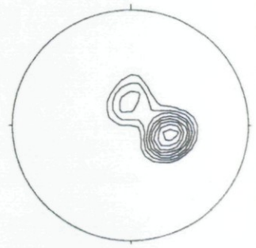

30 data Contoured 2 3 4.... times uniform

Regional Cleavage

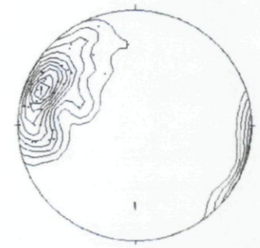

47 data contoured 1, 2, 3..times uniform

LEGEND

- Trend and plunge of minor folds
- Younging direction
- Mineral lineation L_1
- Elongation lineation L_1
- Schistosity
- 70 Cleavage S1 (inclined)
- Cleavage S1 (vertical)
- Lithological boundary
- Normal Fault
- Thrust Fault (inferred)
- Thrust Fault (mapped)
- Anticline
- Syncline
- Shear zone
- Roads
- Creeks

STRATIGRAPHIC COLUMN

- Talisker pyrite unit
- Backstairs Passage Fm
- Brachina Fm
- Tarcowie Siltstone
- Brighton Limestone
- Tapley Hill Fm
- Sturt Tillite
- Belair Subgroup
- Stonyfell Quartzite
- Aldgate Sandstone
- Barossa Complex Basement

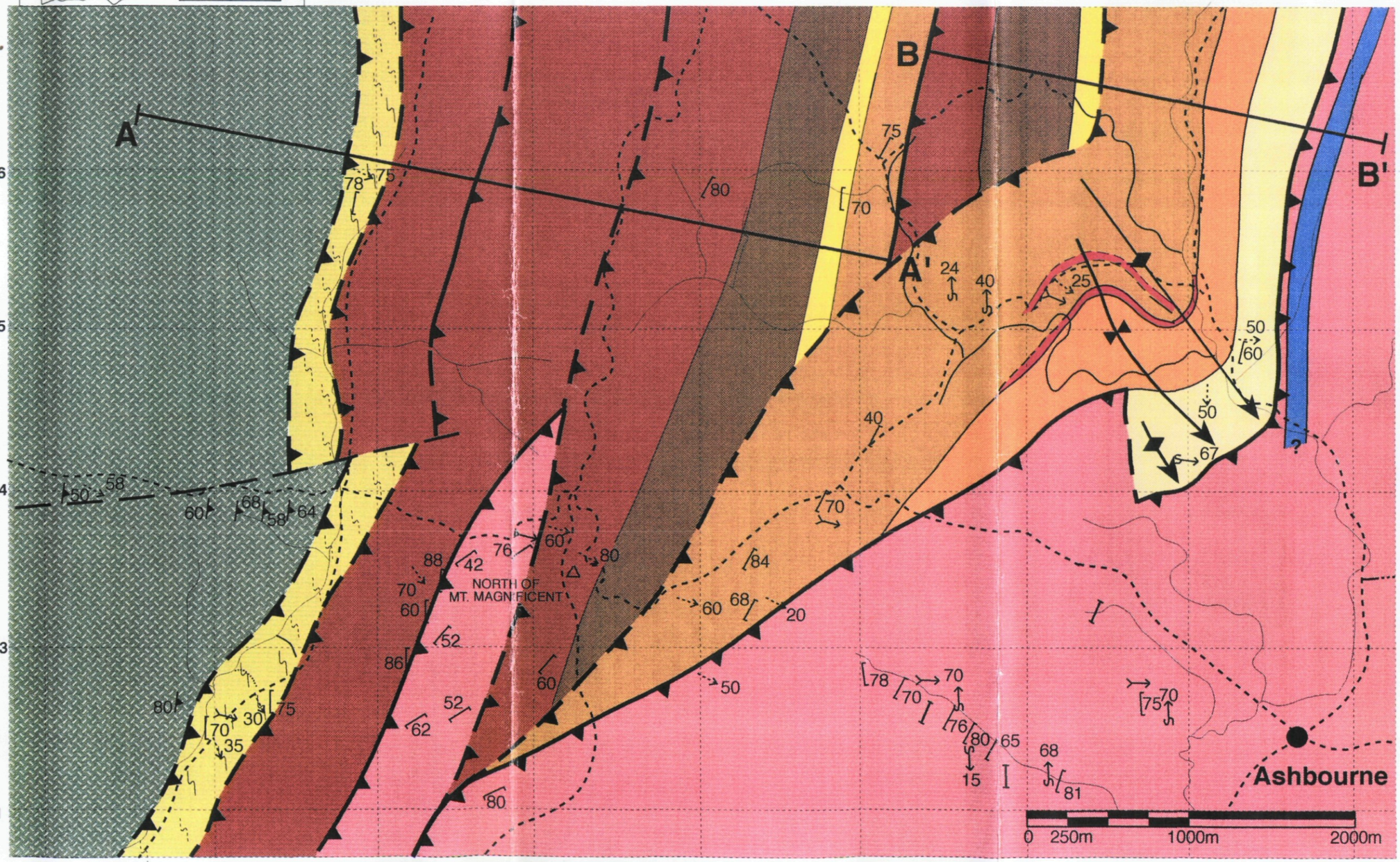

Peta Saunders 1993

THE STILL RANGE IMBRICATE FAN

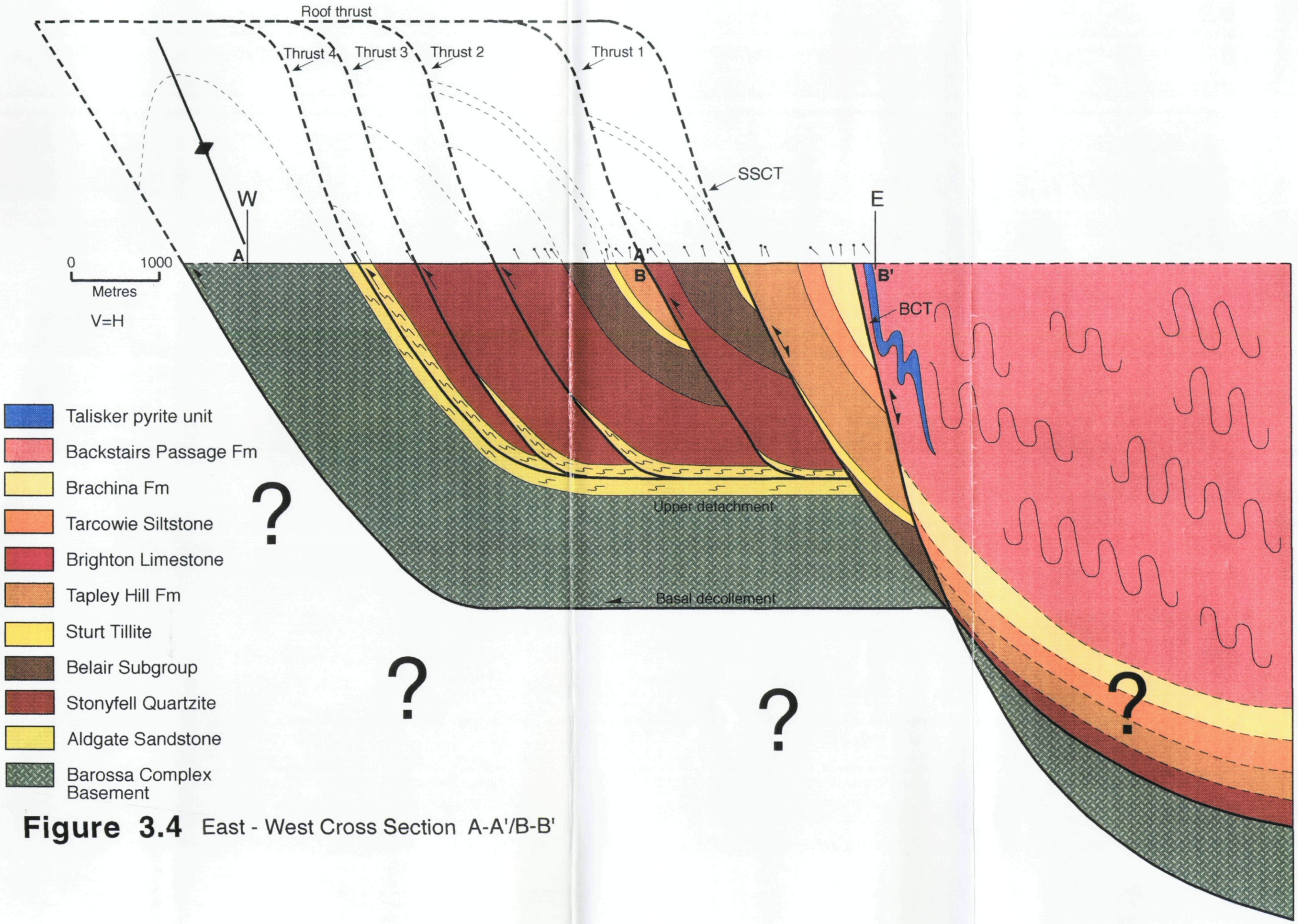

Figure 3.4 East - West Cross Section A-A'/B-B'

Plate 1 Photomicrograph of basement showing retrogressed garnet (isotropic mineral) sericite (yellow) and quartz showing undulose extinction. The schistosity of the basement is defined by micaceous minerals through the centre.(TS A1011-1). Field of view 1.5mm.

Plate 2 Basal conglomerate of the Aldgate Sandstone from the northern area of the BCSZ. View to the north, note lens cap for scale.

Plate 3 Basal conglomerate of the Aldgate Sandstone from the southern section of the BCSZ. Conglomerate unit overlies sandstone unit, pencil for scale is aligned parallel to the main foliation which is at a steeper angle than bedding.View to the south.

Plate 4 Tapley Hill Formation shows pelitic (blue) and psammitic (cream) laminations. Note the microfaults offsetting laminations. Pencil for scale.

Plate 5 Recrystallised Brighton Limestone from folded zone, calcite grains have been strained. Cleavage planes can be seen in individual grains. Field of view 1.5mm.

Plate 6 Porphyroblast in basement with magnetite inclusion trails preserving an earlier fabric. Chlorite minerals surrounding porphyroblast define the major schistosity within the basement. Field of view is 1.5mm TS A1011-114 (YZ section).

Plate 7 Mylonite shows elongation of quartz grains and fine grained recrystallised feldspars. Field of view is 1.5mm TS A1011-107 (XZ section).

Plate 8 Sturt Tillite shows dominant fabric horizontally. Pull apart clast is seen in the centre. Field of view is 1.5mm TS A1011-79 (XZ section).

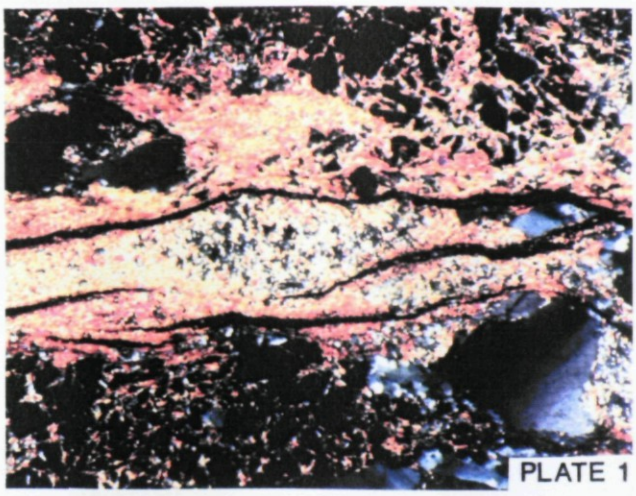

PLATE 1

PLATE 2

PLATE 3

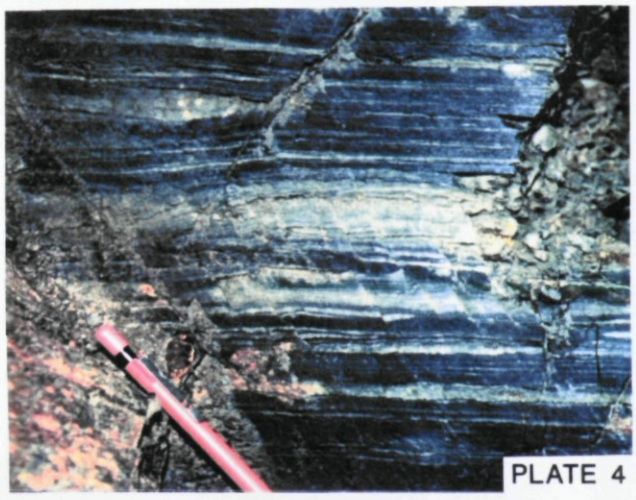

PLATE 4

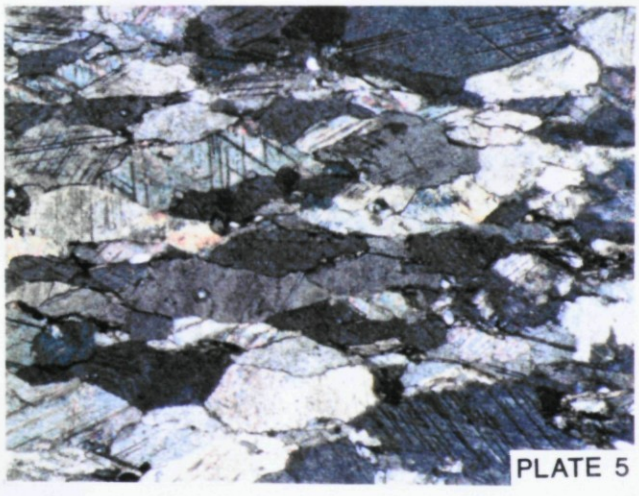

PLATE 5

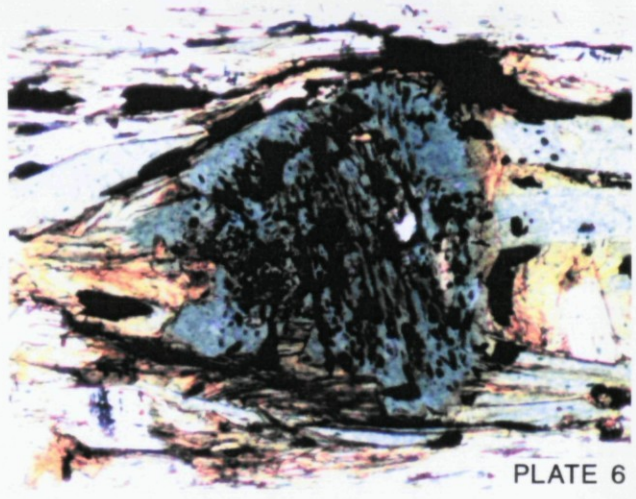

PLATE 6

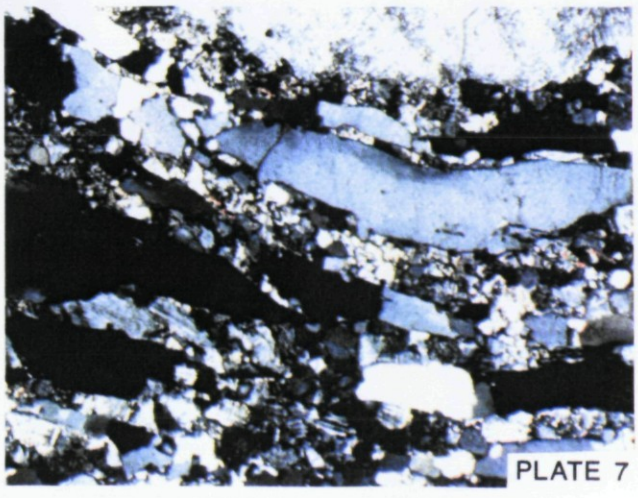

PLATE 7

PLATE 8

Plate 9 Solution cleavage developed in the Tapley Hill Formation. Field of view 1.5mm A1011-71 (XZ section).

Plate 10 Cleavage bedding relationship in the Tapley Hill Formation. Cleavage is defined by micas which are horizontal. Bedding is defined by the quartz rich band at 40° to bedding. Field of view is 1.5mm Al011-71 (XZ section).

Plate 11 Elongation lineations within the Stonyfell Quartzite. Note pen for scale.

Plate 12 Kinking in the Stonyfell Quartzite. Photo is taken east (left), west (right). Field of view is 6 metres.

Plate 13 Crystal plastic deformation leading to grain boundary suturing in the Stonyfell Quartzite. Field of view is 1.5mm A1011-95 (XZ section).

Plate 14 Subgrain formation as a result of high strain leading to crystal plastic deformation in the Stonyfell Quartzite. Field of view is 1.5mm A1011-20.

Plate 15 Folding within the calcareous unit of the Tapley Hill Formation. Lens cap upper left corner for scale.

Plate 16 Tight chevron folds within the Brachina Formation. Pencil for scale.

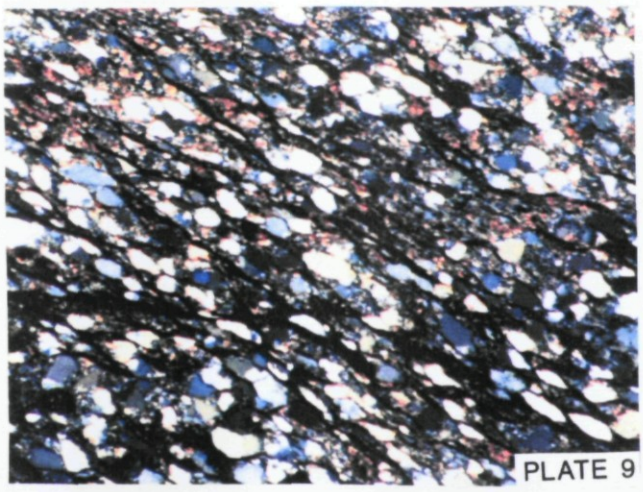

PLATE 9

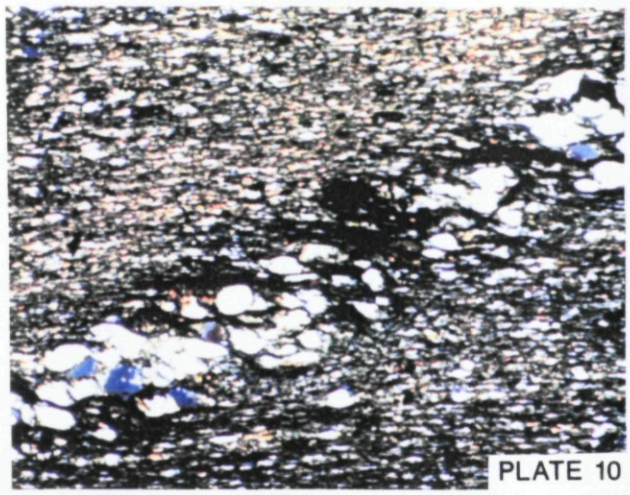

PLATE 10

PLATE 11

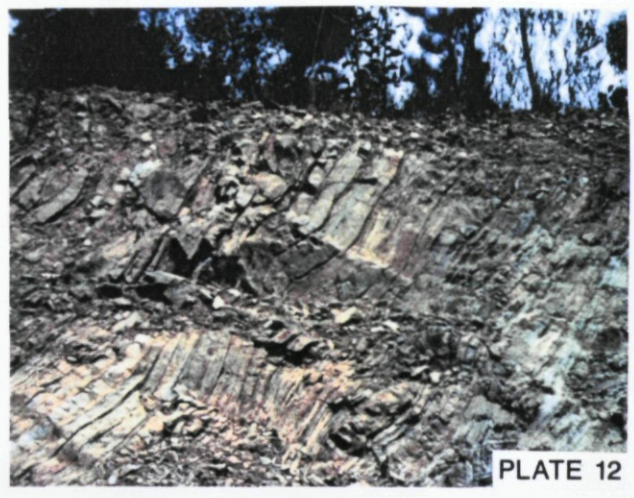

PLATE 12

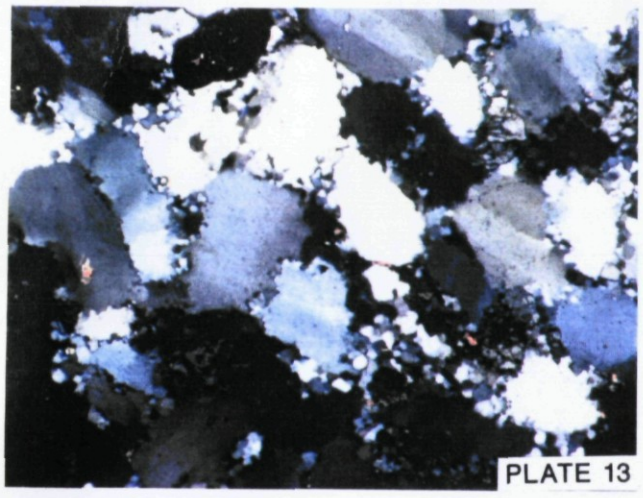

PLATE 13

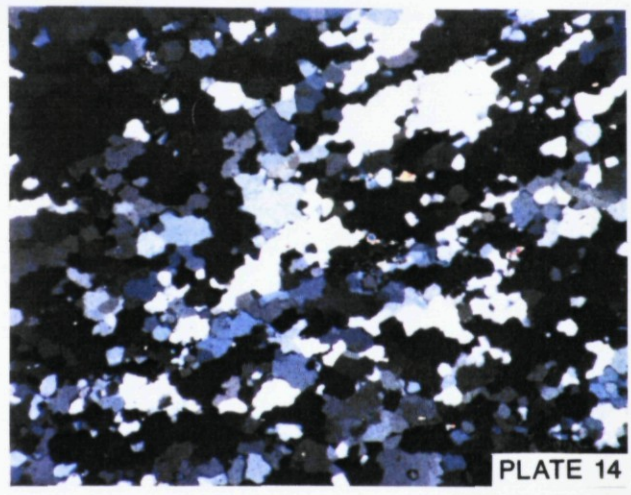

PLATE 14

PLATE 15

PLATE 16

Plate 17 Conjugate kink folds in the Brachina Formation. Pencil for scale.

Plate 18 Microscopic conjugate kink folds within the Brachina Formation. Fabric is defined by micaceous minerals. Note the presence of the euhedral magnetite grains. Field of view is 1.5mm.

Plate 19 Box fold formed within the Brachina Formation. Geopick for scale.

Plate 20 Reverse fault displacing beds of the Backstairs Passage Formation. Lens cap top left corner for scale.

Plate 21 Class 2 similar fold within the Backstairs Passage Formation. Geopick handle or scale.

Plate 22 Reflected light photomicrograph of the basement. Magnetite appears white and silicate minerals form the grey matrix. Magnetite preferentially aligned parallel to the dominant schistosity. Field of view 1.5mm TS A1011-130.

Plate 23 Large euhedral grain of magnetite within the Brachina Formation, associated with quartz veining. Viewed under transmitted light. TS A1011-30 field of view is 1.5mm.

Plate 24 Large euhedral grain of magnetite (responsible for high magnetic susceptibility) shows very slight martitisation along octahedral cleavage faces. Fine grained magnetite (white) parallels the dominant foliation. Viewed under reflected light. Field of view 0.15μm TS A1011-30.

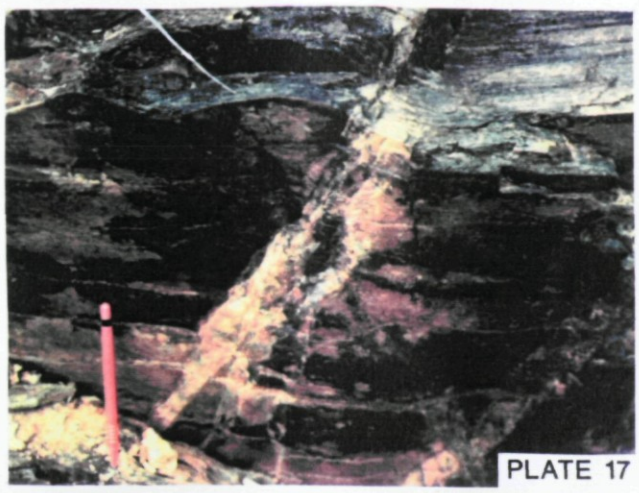

PLATE 17

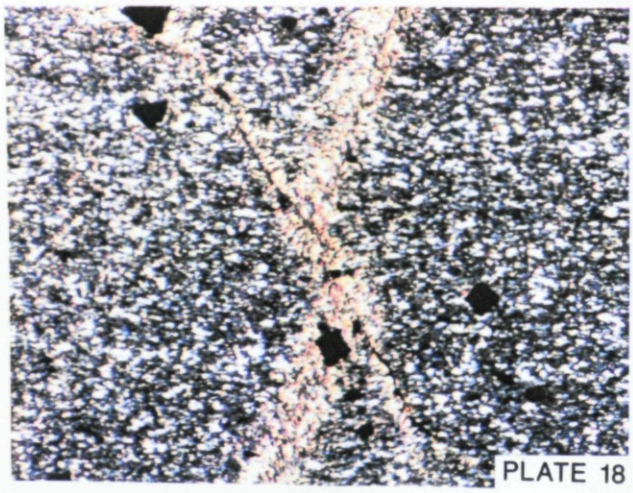

PLATE 18

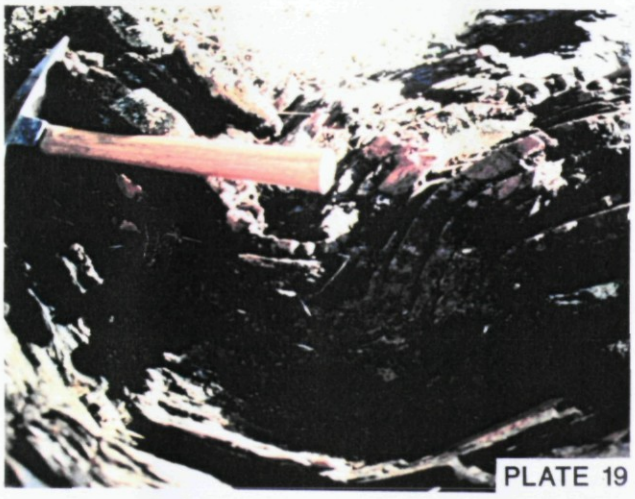

PLATE 19

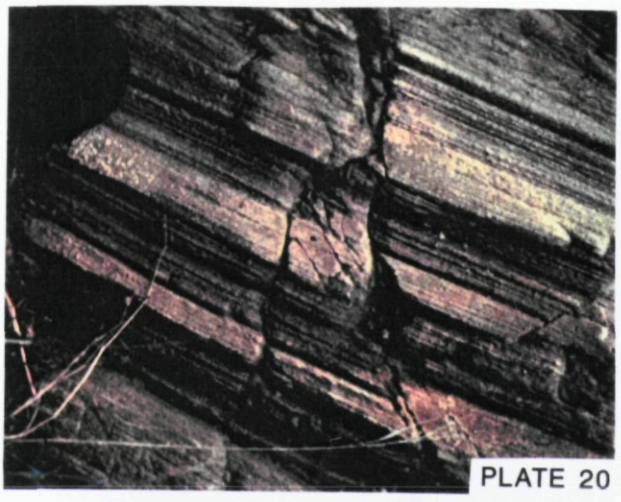

PLATE 20

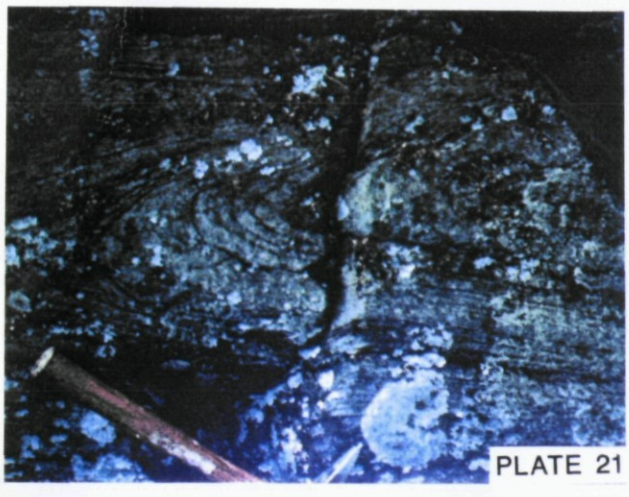

PLATE 21

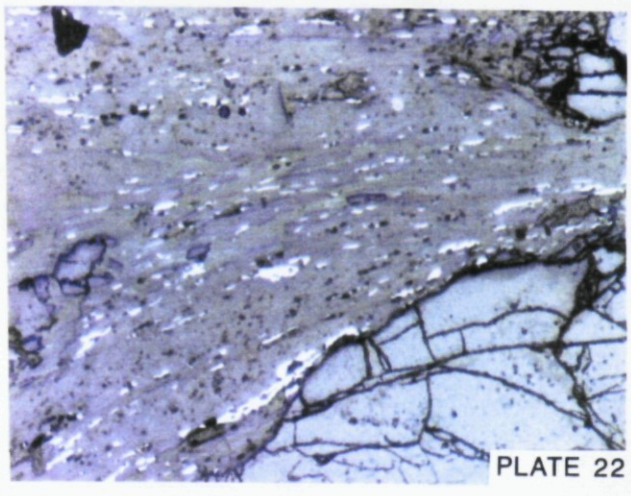

PLATE 22

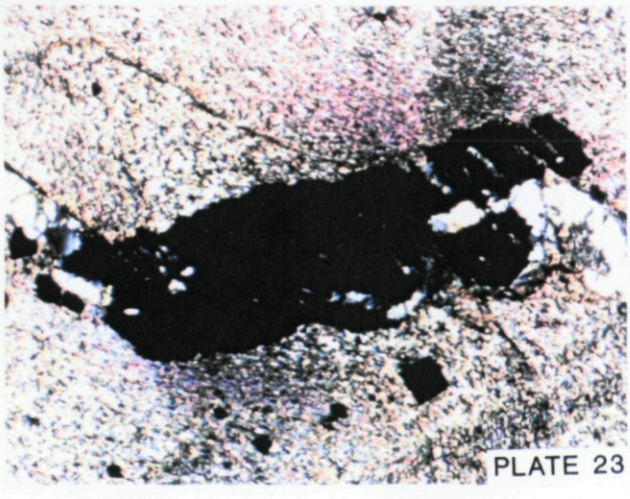

PLATE 23

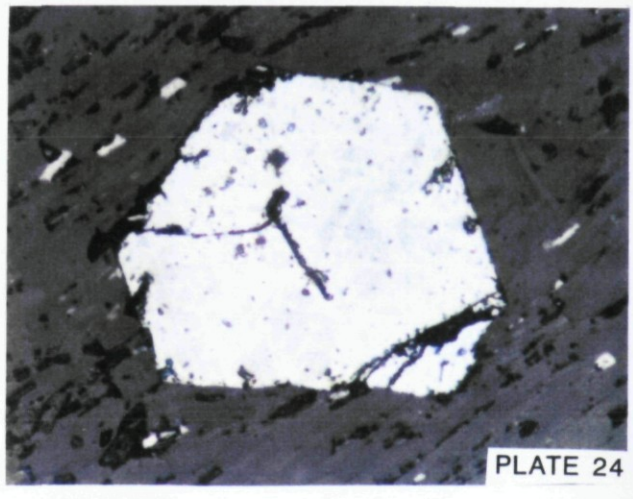

PLATE 24

4. GEOPHYSICAL INTERPRETATION

4.1 The Magnetic Method

Airborne magnetic surveys record geomagnetic intensity (Telford, 1990). This includes signal from the rock units below, the earth's main magnetic field, diurnal variations (daily variation related to solar activity) and cultural (non-geological) noise. The removal of the sources of noise results in a residual reading. This is equal to that of the rock units below, from this magnetic units within the crust may be identified.

The data used in this study is part of the Bull Creek high resolution aeromagnetic survey which was flown for CRAE in 1979. Flight lines are 300 metres apart and run East-West, with sampling every 25 metres along these lines. The sensor height of the magnetometer was 80 metres above ground. The magnetic signal has already been corrected and data obtained indicates the amplitude of magnetic anomalies from the earth's crust.

Magnetic anomalies arise through the varying distribution of magnetic minerals within the earths crust. In a magnetic survey information is obtained from depths down to 20km, which is the approximate location of the Curie Point isotherm of 550°C. At higher temperatures than this minerals lose their magnetic properties. The major magnetic minerals in metasediments are magnetite and pyrrhotite (Grant 1984, Telford, 1990). Their presence or absence depends primarily upon the bulk composition of the sediments prior to metamorphism, oxidation state and the degree of metamorphism (Rumble, 1973). This leads to the uneven distribution of these minerals and means that they are not necessarily confined to stratigraphic or lithological boundaries.

The effective display of data is essential, as geological interpretation is based upon this (Boyd, 1967 and Rajagopalan and Boyd, 1987). Aeromagnetic data has been filtered in various ways to enhance features. For better definition of the edges of anomalies a vertical gradient filter developed by Paine (1985) has been applied (Nelson 1988). To amplify the effects of weak signals an AGC filter has been used. Most anomalies of the Bull Creek survey are at (or very close to) the surface and yield high frequency anomalies (Figure 4.1).

Data has been displayed as contour maps (Figure 4.3) and stacked profiles (Figure 4.4 and 4.5) for quantitative interpretation and as greyimages (Figure 4.2 and 4.7a) for qualitative interpretation. Contour maps produced from aeromagnetic data are used to define the location and relative intensity of anomalies. Individual profiles were used in magnetic interpretation to

locate magnetic anomalies accurately and determine width, depth to the top of magnetic units and provide dip estimates, through modelling programs.

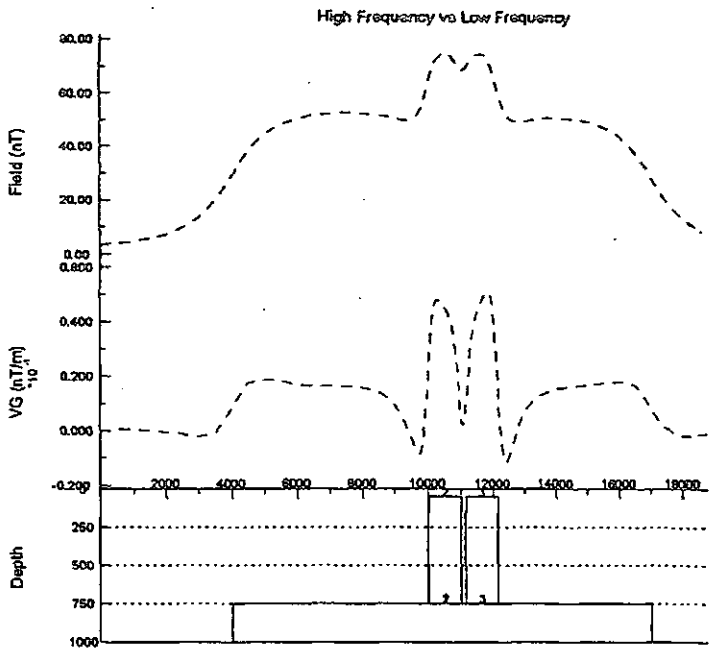

Figure 4.1 The top signal represents the Total Field anomaly which would result from the magnetic bodies below. The bottom signal represents the anomaly of the same magnetic unit after it has been passed through a vertical gradient filter. The vertical gradient defines the edges of anomalies, enhances the effects of shallow sources (bodies 2 and 3) and distinguishes between close sources.

The interactive magnetic anomaly modelling program, GAMMA (developed by Paine, 1985) has been used to provide constraints on the geological interpretation of magnetic bodies at depth. It is important to note that modelling does not necessarily reveal the exact nature of fault or lithological boundaries as magnetic minerals contributing to the signal are not always confined to these boundaries. In the study area however it appears that most anomalies correlate well with mapped geological features, which are either lithological, fault or fold boundaries (Figure 5.1 and 5.1a). The nature of more simple Adelaidean and Kanmantoo profiles have been investigated. Anomalies have been modelled from Total Field and more importantly VG profiles (Figure 4.5). Basement anomalies have not been modelled as the basement consists of many individual anomalies which are not continuous linear features as the distribution of magnetic minerals is complex.

Figure 4.2 Greyscale image of total magnetic intensity for the Bull Creek area. The map scale is 1:50 000 and shows magnetic highs in black and magnetic lows in white.

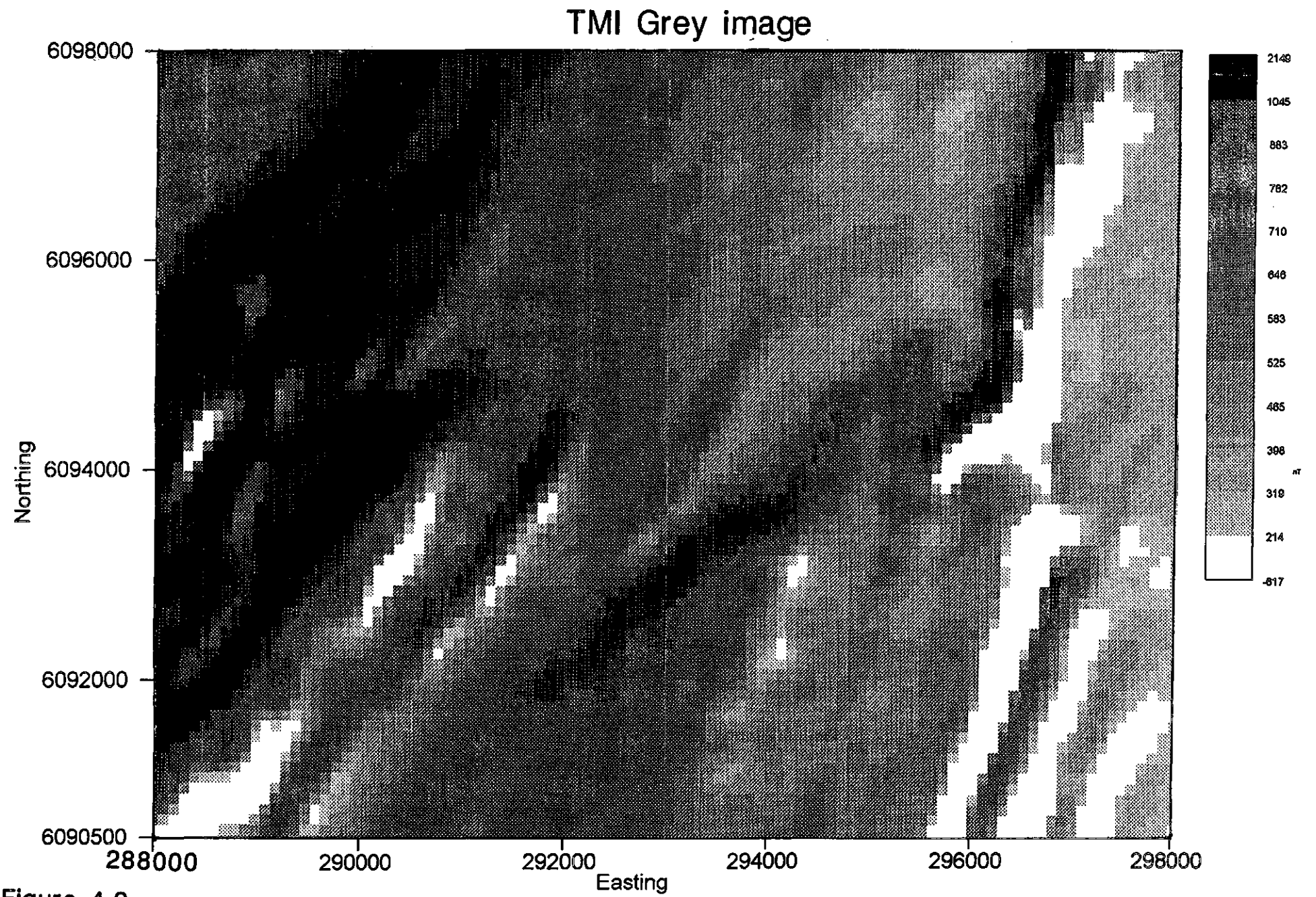
TMI Grey image
6098000
6096000
6094000
6092000
6090500
Northing
288000
290000
292000
294000
296000
298000
Easting
2149
1045
883
782
710
646
583
525
465
398
319
214
-617
nT

Figure 4.2

Figure 4.3 TMI contour map of the Bull Creek study area. Map scale is 1: 50 000, contour intervals are 10 nT. All units describe a magnetic high except for the far right anomaly (Unit 5C) which is negative.

Figure 4.3a The transparency outlines the lithomagnetic units described in the text.

Unit 1: Basement
Unit 2: Stonyfell Quartzite
Unit 3: Tapley Hill Formation
Unit 4: Brachina Formation
Unit 5A: Backstairs Passage Foramtion (Ashbourne Wedge)
Unit 5B: Backstairs Passage Formation (Mt. Magnificent Re-entrant)
Unit 5C: Talisker equivalent ?

Solid lines indicate magnetic anomalies identified on the Figure 4.2 TMI Contour map. Dashed lines indicate anomalies identified from AGC stacked profiles and the grey image.

Magnetic Interpretation Map

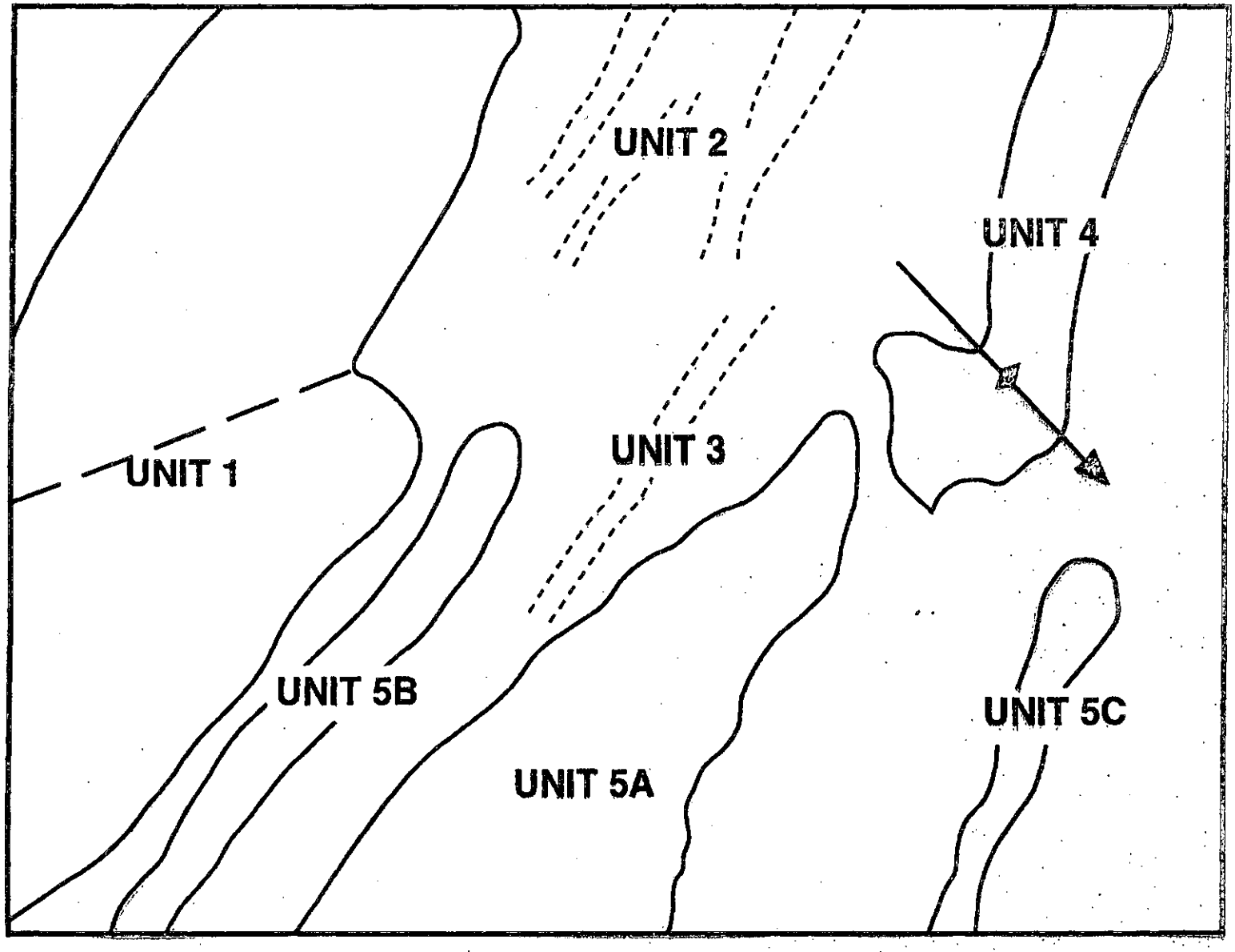

Figure 4.3a

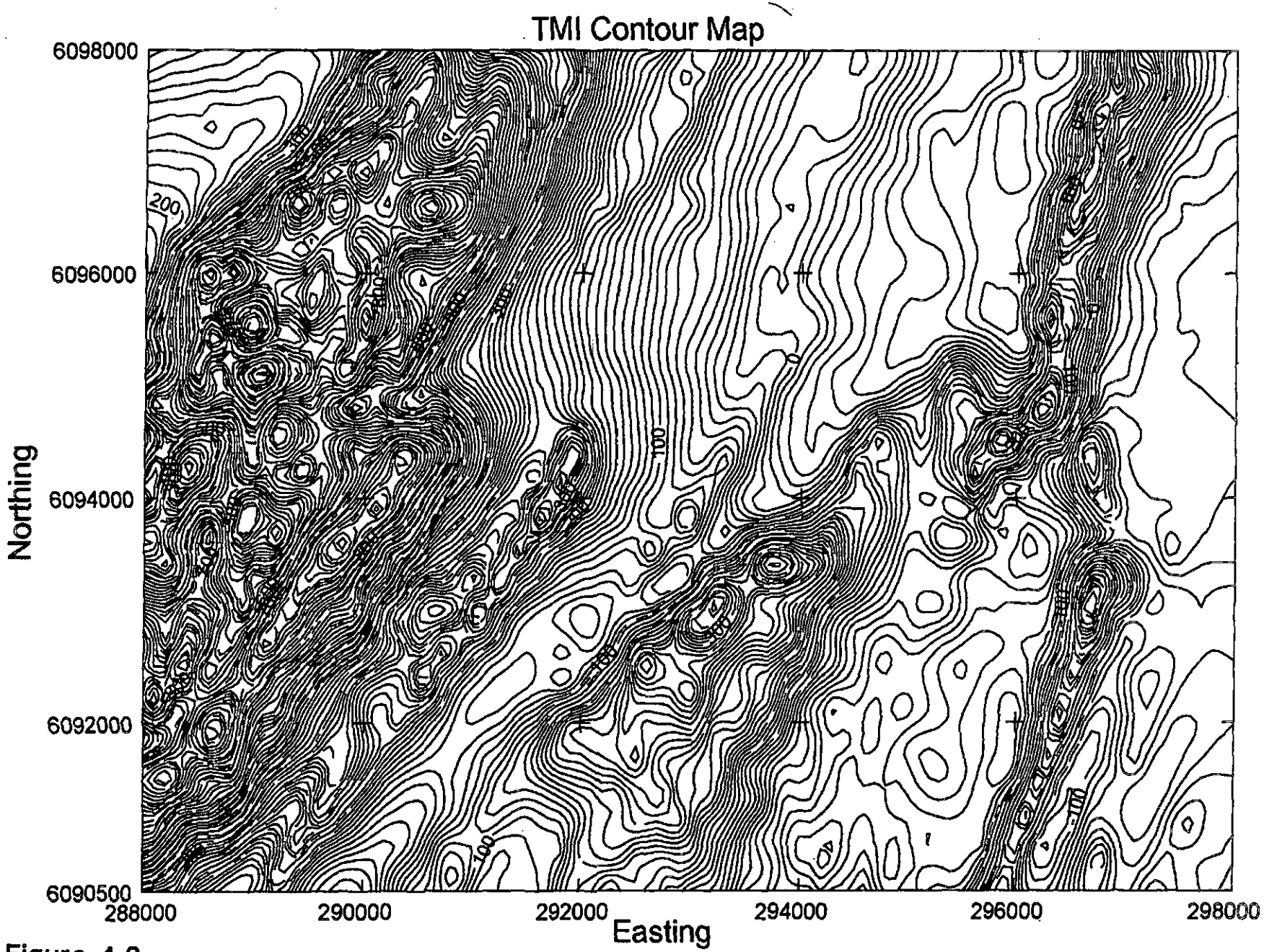
TMI Contour Map
6098000
6096000
6094000
6092000
6090500
Northing
288000
290000
292000
294000
296000
298000
Easting

Figure 4.3

Figure 4.4 Stacked profiles have been generated from magnetic data collected along survey flight lines. The stacked profile map shown has been passed through an AGC filter and is presented at a 1:50 000 scale. Note the linear anomalies which may be traced. Anomalies may be accurately located in their position at the surface on these stacked profiles.

Figure 4.4a The transparency outlines the lithomagnetic units described in the text.

Unit 1: Basement
Unit 2: Stonyfell Quartzite
Unit 3: Tapley Hill Formation
Unit 4: Brachina Formation
Unit 5A: Backstairs Passage Foramtion (Ashbourne Wedge)
Unit 5B: Backstairs Passage Formation (Mt. Magnificent Re-entrant)
Unit 5C: Talisker equivalent ?

Solid lines indicate magnetic anomalies identified on the Figure 4.2 TMI Contour map. Dashed lines indicate anomalies identified from AGC stacked profiles and the grey image.

Magnetic Interpretation Map

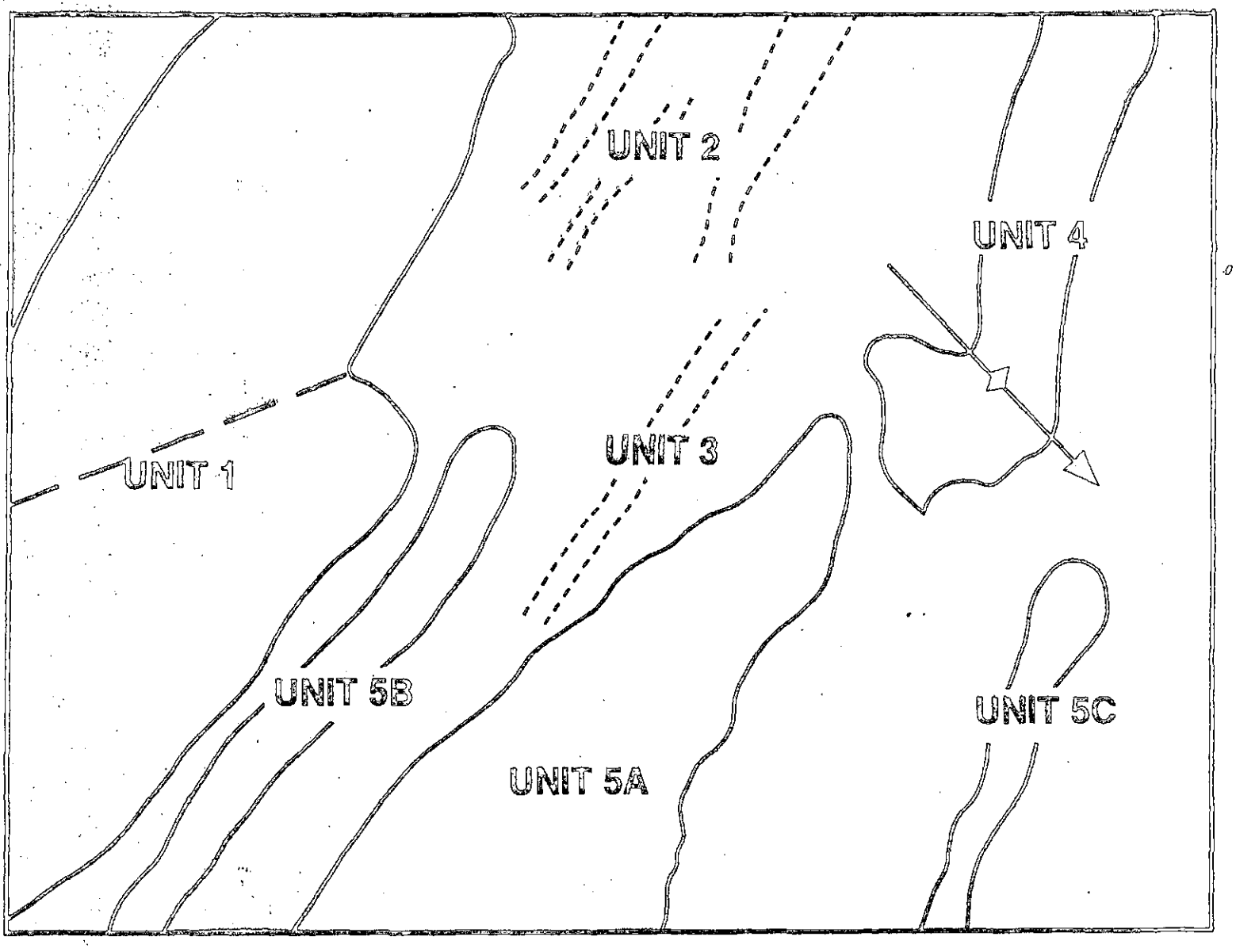

Figure 4.3a

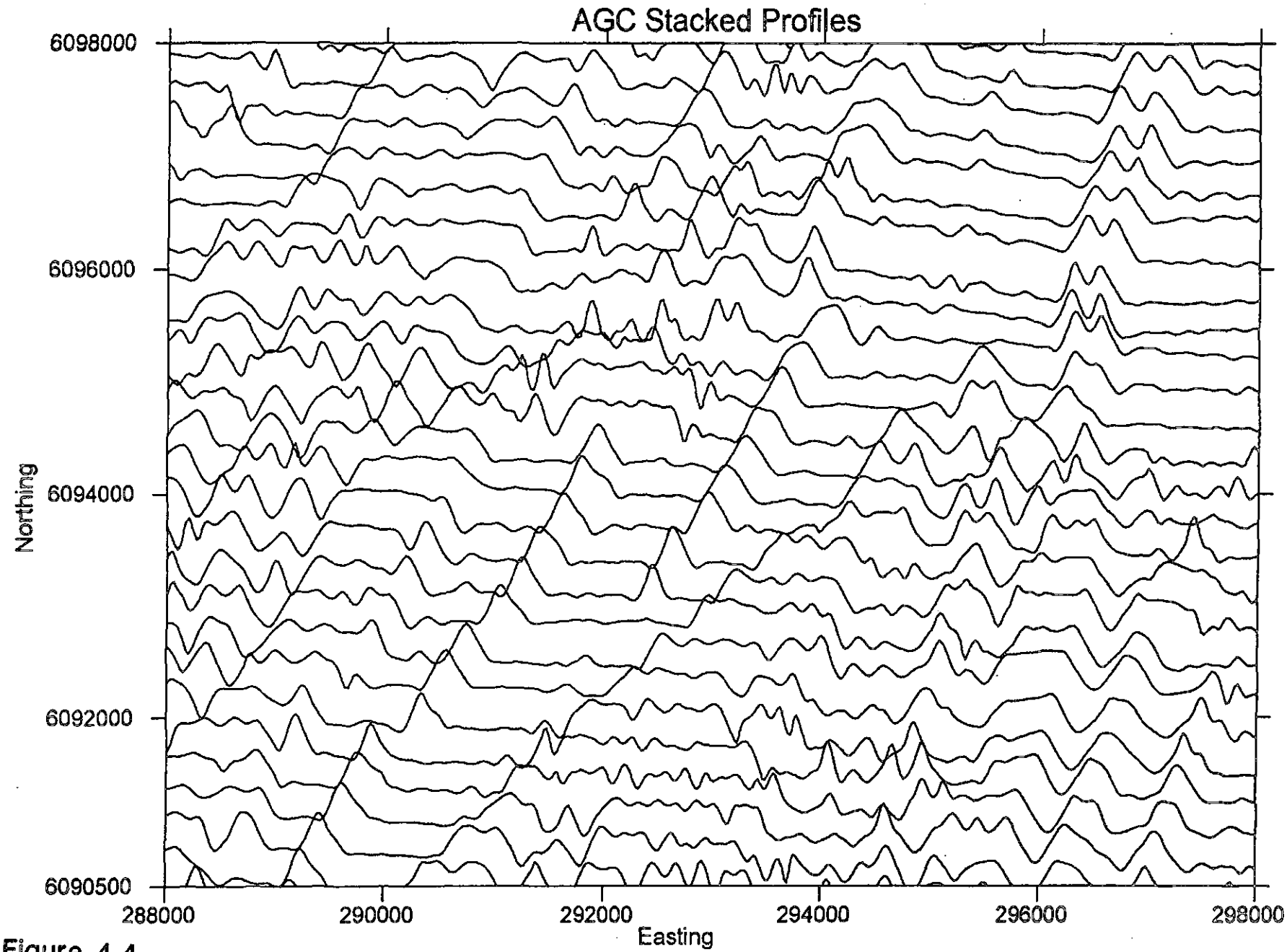
AGC Stacked Profiles
6098000
6096000
6094000
6092000
6090500
Northing
288000
290000
292000
294000
296000
298000
Easting

Figure 4.4

Figure 4.5a Stacked Profile map of magnetic anomalies passed through a vertical gradient filter. Highlighted anomalies have been modelled and the results of modelling are shown in figures 4.5b,c and d.

Figure 4.5 (b-d) The solid lines show real data from the Bull Creek area TMI (top) and VG (bottom) anomalies. The dashed lines show calculated TMI and VG anomalies which result from the magnetic bodies shown below the surface. All calculated and real anomalies correlate well with steep easterly dipping lithomagnetic units.

The most easterly anomaly of Figure 4d is a large negative anomaly shown to be a steep easterly dipping anomaly which has a large negative susceptibility attributed to NRM.

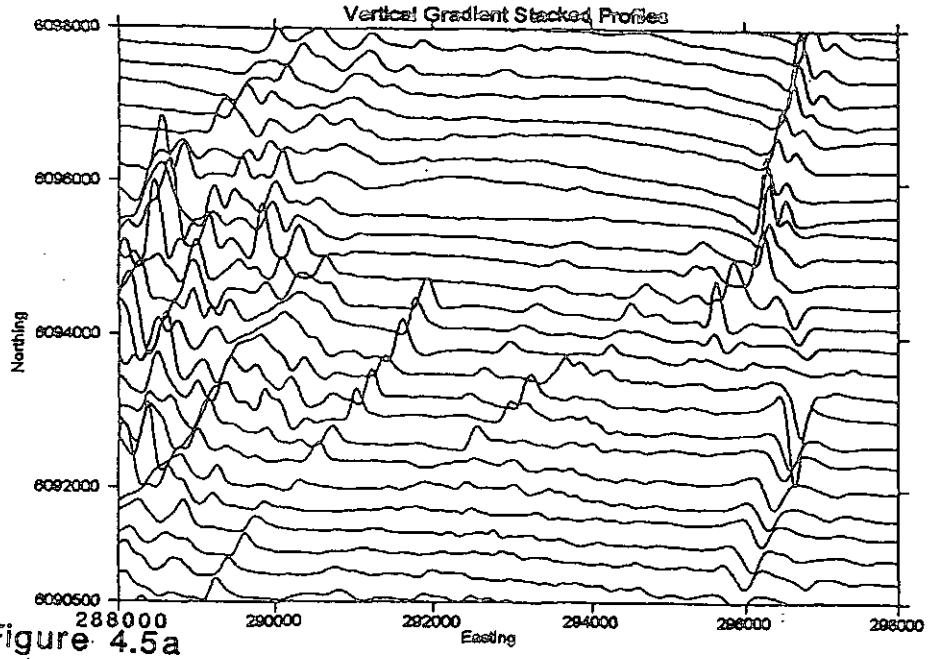

Figure 4.5a

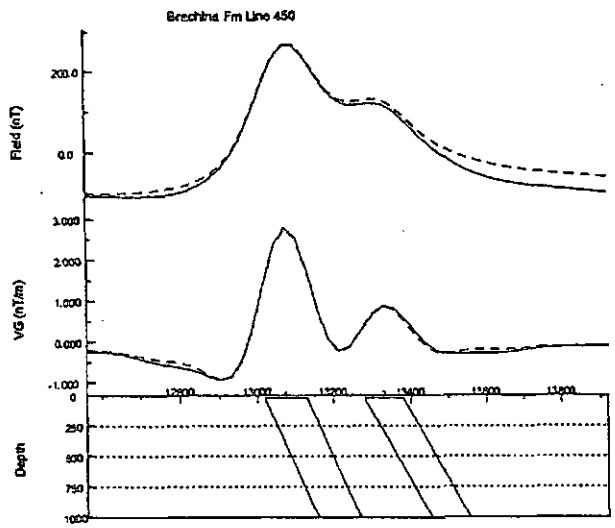

Figure 4.5b

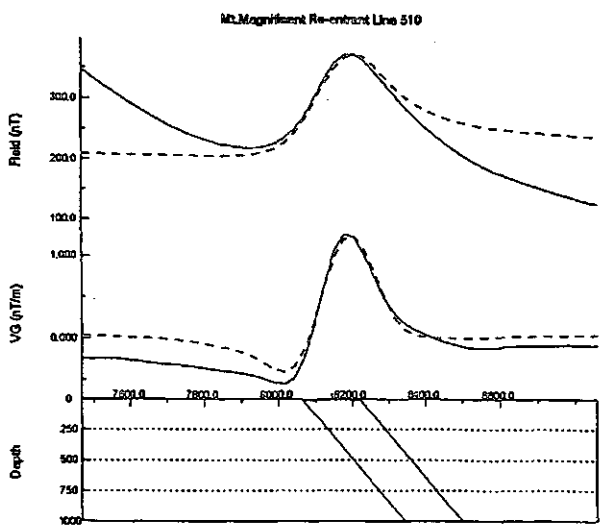

Figure 4.5c

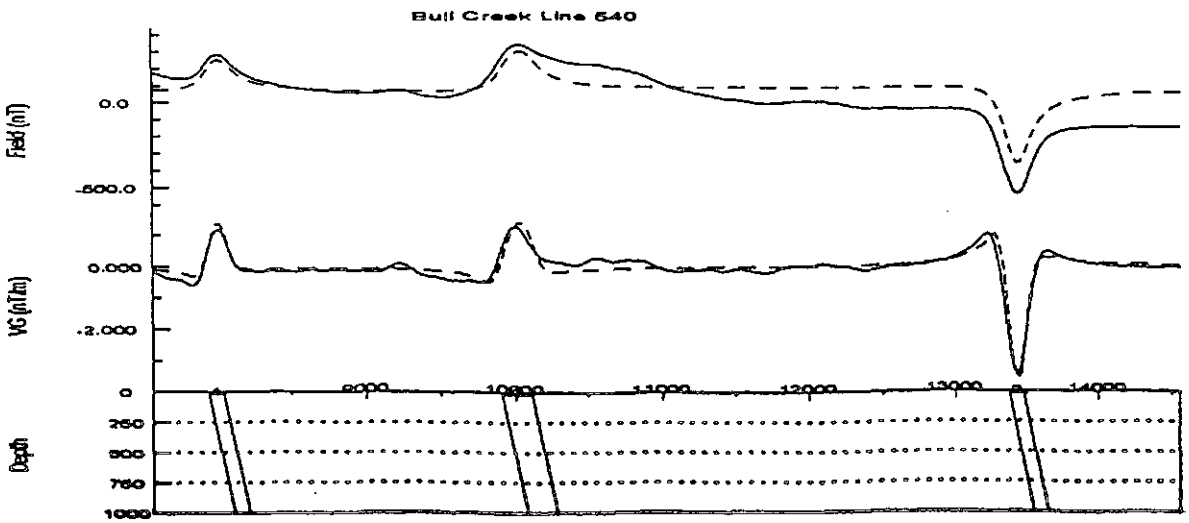

Figure 4.5d

The magnetic mineral content of the outcropping lithomagnetic units were examined in polished thin section under a reflected light microscope, descriptions are given in Appendix 1. Susceptibility readings were taken to match lithological units to magnetic anomalies.

4.2 Radiometric Analysis

Radiometric and aeromagnetic data are recorded synchronously during airborne surveys. Data is recorded by a gamma ray scintillation detector as counts per second (CPS). Radiometric data does not provide three dimensional constraints on structural geometry as magnetics does, but it provides two dimensional constraints on lithology, as gamma ray emission is from the top 50cm only. Although there is little outcrop in the study area, the soil cover is a direct indicator of the rocks (which are very close to the surface) below, and the signal obtained reflects lithology.

The radiometric signal is produced by the contribution of gamma ray emissions from the radioactive decay of elements. Those elements which contribute most of the gamma ray emissions are potassium, uranium and thorium (Telford, 1990). In crustal rocks potassium forms one of the major elements incorporated into minerals. The intensity of the signal obtained reflects the concentration of that particular element in the lithologies below. The signal only involves input from the top 50cm whether this is the weathered zone or rock outcrop.

Feldspars, micas and other potassium rich minerals are the most common source of radiometric highs. Total count (encompassing gamma ray contributions from all elemental decay reactions), uranium and thorium data were collected in the Bull Creek survey. Due to processing errors the potassium channel was not obtained, however the total count encompasses signal from the potassium decay reactions so its relative abundance is included. The uranium and thorium are present in very small quantities and do not reveal any more information than the total count in this study. Therefore all radiometric interpretation has been carried out on total count data. The radiometric image (Figure 4.6) displays prominent NE-SW trends similar to the magnetic map.

The magnetic and radiometric response of the various stratigraphic units was examined (Figure 4.7a and b). The two images (Figure 4.7a and b) show very good correlation with prominent NE-SW striking anomalies observed on both maps. The geophysical response of stratigraphic units is described and the lithomagnetic units and radiometric signal within these are discussed below.

Figure 4.6 Total count radiometric greyscale image at 1:50 000 scale shows prominent NE-SW trends indicative of the strike of the lithologies below. The black areas show high count rates and white areas show low count rates

Figure 4.6a The transparency shows interpreted boundaries which are divided into units which correspond to the assigned magnetic units.

Interpretation Map

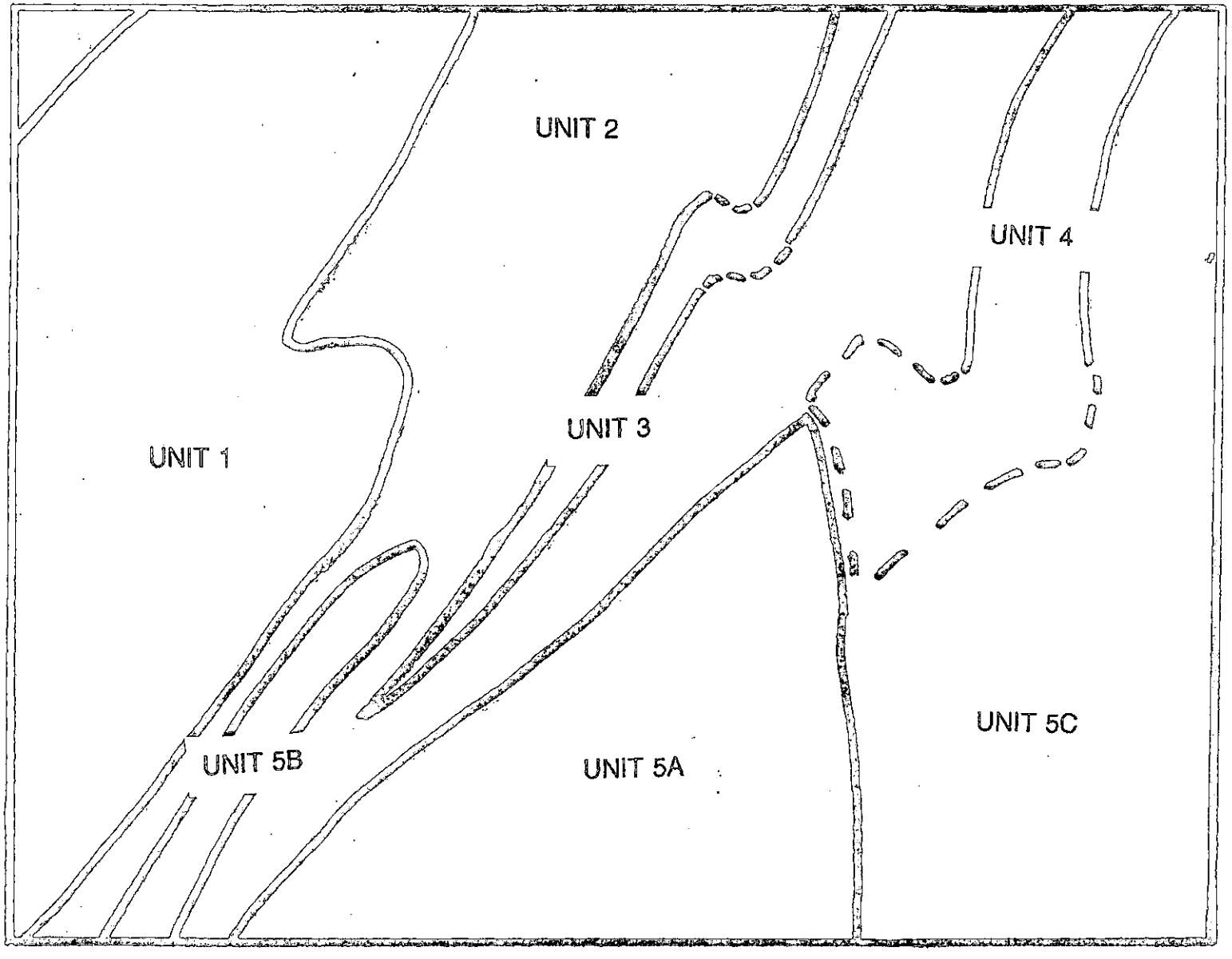

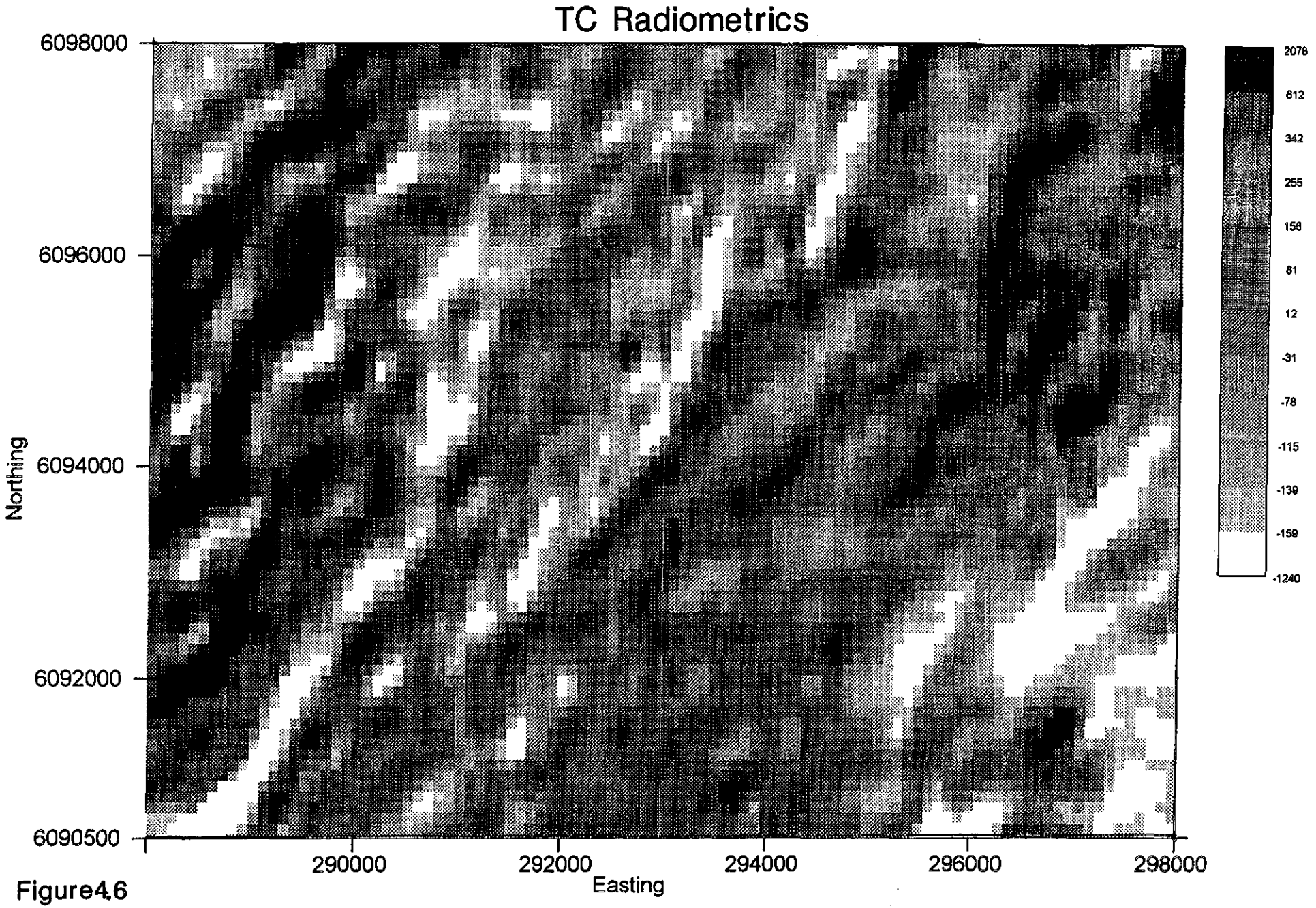
TC Radiometrics
6098000
6096000
6094000
6092000
6090500
Northing
290000
292000
294000
296000
298000
Easting
2078
612
342
255
158
81
12
-31
-78
-115
-139
-159
-1240

Figure4.6

Figure 4.7a Shows a **magnetic** VG greyimage at a 1:100 000 with a 45° sun angle applied.

Figure 4.7b Shows a **radiometric** TC grey image at a 1:100 000 (grey scale legend units are in CPS).

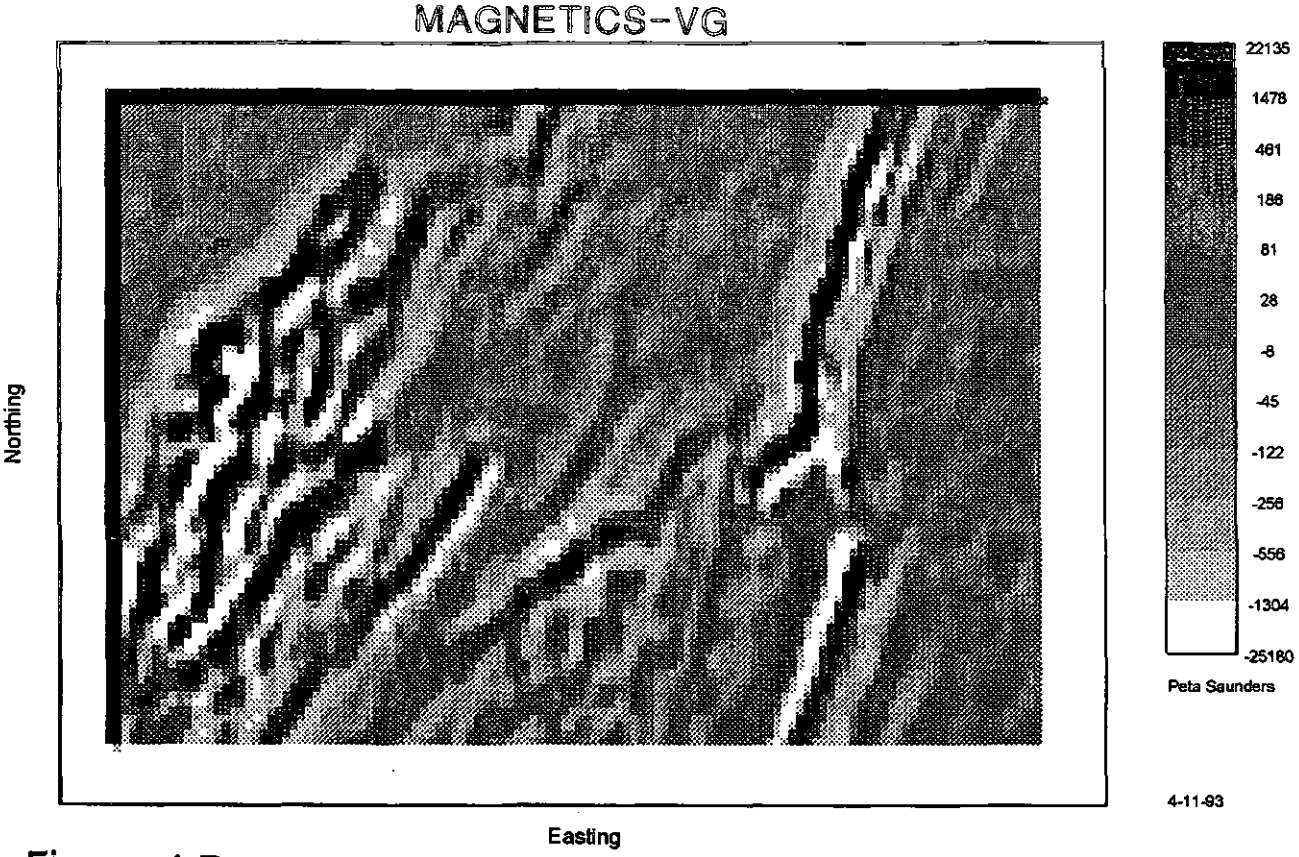

Figure 4.7a

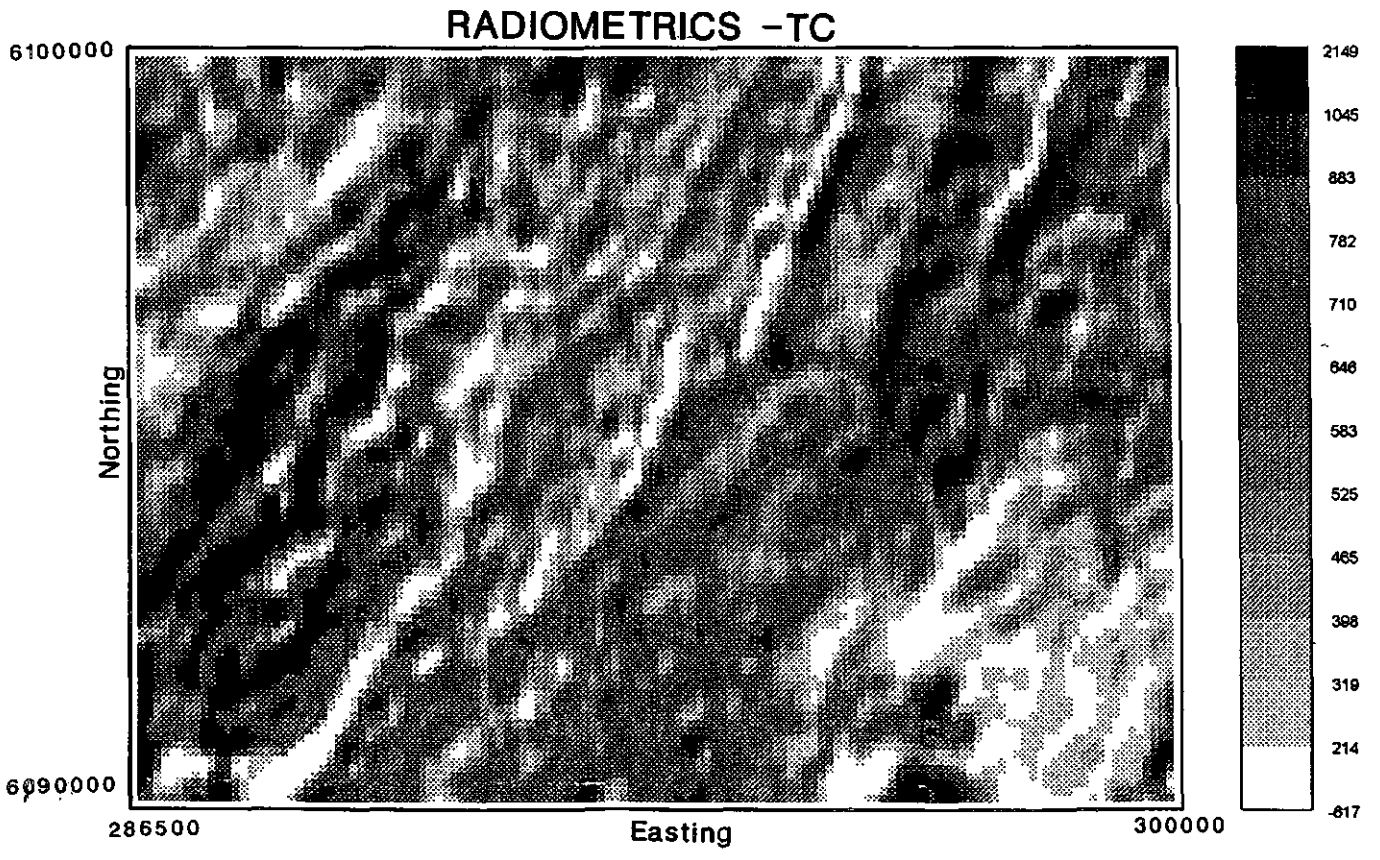

Figure 4.7b

4.3 Geophysical response

UNIT 1 Basement

The magnetic anomalies associated with the basement vary in intensity from 650-1200nT. The basement signal is erratic and considerable variation in anomalies is observed (especially the stacked profiles of Figure 4.4 and 4.5) which reflects the inhomogeneous distribution of magnetic minerals. Polished thin section examination reveals the presence of fine grained magnetite which is responsible for the anomalous high of the basement. The preferred alignment of magnetite suggests that it has replaced biotite in the manner suggested by Grant (1984), taking on the grain structure and orientation of the biotite which it has replaced. Between 10 and 50 susceptibility readings were taken at outcrops with values averaging 200-300 x 10^{-5} S.I. units. These values appear too low, this may be explained by limited sampling (due to poor exposure) and the highly weathered nature of outcrop. The basement anomaly is offset by a fault through the middle (previously interpreted by Rajagopalan, 1989) which displays apparent sinistral displacement. This is best observed on the TMI contour map of Figure 4.3.

The basement displays the highest radiometric values due to the potassium rich nature. It has been suggested that the basement has granitic origins, this is supported by the high total count reading which indicates it is rich in potassium, as is expected if it is a felsic crustal rock. The feldspar minerals have subsequently degraded and potassium is now found in muscovite and retrograde minerals such as sericite.

UNIT 2 Stonyfell Quartzite

The AGC filter enhances a group of small anomalies in the central northern area (Figure 4.4). These anomalies are small and occur within the Stonyfell Quartzite. As there is no outcrop in the area the source of these anomalies cannot be found. It is likely that they result from magnetite occurring as heavy mineral bands within the Stonyfell Quartzite. However they may possibly be the result of underlying basement which is close to the surface.

UNIT 3 Tapley Hill Formation

The dominant radiometric low in the area follows the Tapley Hill Formation unit which appears to strike NE-SW through the central area. This unit is calcareous and lacks potassium bearing minerals therefore a radiometric low is observed. This unit appears either folded or faulted in its central area and has been interpreted as a fold on the magnetic interpretation map of Figure 4.3a.

UNIT 4 Brachina Anomaly

The intensity of the Brachina Anomaly varies from 200-300 nT. The Brachina profile has been modelled (Figure 4.5) and is characterised by two peaks indicative of two parallel linear

anomalies which may indicate a less susceptible unit lies between the two. Polished thin section examination reveals two magnetite populations (Plate 23). Fine elongate magnetite grains are aligned parallel to the main slaty cleavage and form the main magnetite population. These have probably formed during metamorphism. Large euhedral grains have grown over the metamorphic fabric, as they show no preferential orientation. These larger magnetite grains are responsible for the high susceptibility of the Brachina Formation and have been martitised to haematite along octahedral cleavage planes (Plate 24). Measurements for susceptibility range from 200-2000 x 10^{-5} S.I. units which is high.

Radiometric analysis of the Brachina Formation reveals a high count rate. The unusual termination of the Brachina is defined but not as well as with the magnetic data. This may be due to the contribution of weathered material which has moved from its source area.

UNIT 5A Ashbourne Wedge anomaly

Unit 5A comprises a zone of erratic signals which have a distinct Eastern boundary (interpreted as a fault boundary). Examination of the opaque minerals reveals fine grained magnetite which replaces biotite. Magnetic susceptibilities range from 500-1000 x 10^{-5}S.I. units which is quite high and confirms that the aeromagnetic anomaly results from the high magnetic susceptibility of this unit present in outcrop.

UNIT 5B Mt. Magnificent Re-entrant

The vertical profile consists of one linear anomaly which has been modelled (Figure 4.5c, for location see Figure 4.5a). Suprisingly the outcrop of this unit does not yield high susceptibility values, suggesting a deeper magnetic source. However this source could not be much deeper as it is a high frequency signal attributed to shallow sources. Measurements taken may not be truly representative as the outcrop is limited and only a few susceptibility measurements were taken. A possible source for this magnetic anomaly may be alternatively attributed to a concentration of highly susceptible magnetic minerals along the fault zone.

The Ashbourne Wedge zone and the Mt. Magnificent Re-entrant zone both display similar intermediate signals, which is further evidence to suggest the re-entrant is of the same unit as the wedge.

UNIT 5C Kanmantoo negative anomaly

The very eastern margin of the Ashbourne Wedge is marked by a prominent linear negative anomaly. In this region there is no outcrop due to Permian cover, therefore susceptibility and rock type, of the anomaly, could not be ascertained. Modelling has been carried out on this unit (Figure 4.5d) and a high degree of Natural Remanent Magnetisation has been suggested.

5. INTEGRATED GEOLOGICAL INTERPRETATION

5.1 A Discussion of Geophysical Constraints Upon Structural Interpretation

Structural maps provide a basis for geological interpretations, and with the addition of geophysical data these maps can further be refined. The NE-SW trend of lithologies is evident in both the geophysical and geological maps. Faults are defined, by contrasting lithomagnetic units, rather than magnetic anomalies resulting from the concentration of magnetic minerals within fault zones. Folding of lithomagnetic and radiometric marker horizons of the Tapley Hill Formation is evident in the greyscale images and contour maps. The geophysical interpretation map (Figure 5.1a), combining both aeromagnetic and radiometric data, is overlain upon the geological map and shows good correlation between mapped structures (Figure 5.1) and those interpreted through geophysical data .

The basement boundary is defined by magnetic and radiometric data, which places far better constraints on the boundaries than is possible through field mapping alone. The Kyeema Fault is a prominent feature of geophysical maps, especially the TMI contour map (Figure 4.3). The variable composition of the basement is revealed from both radiometric and magnetic data making the differentiation of chemically and mineralogically distinct zones possible. The detailed chemical and mineralogically information is not obtainable through field sampling, due to sparse outcrop. The stacked profiles (Figures 4.4 and 4.5a) reveal the presence of a low frequency regional high, west of the BCT which is attributed to the basement, however this signal is not observed east of the BCT. This suggests that the basement has been down faulted to the east and is present at a much greater depth below Kanmantoo Group sediments.

A number of small magnetic anomalies attributed to the Stonyfell Quartzite are amplified and defined on the AGC stacked profiles (Figure 4.4). These anomalies confirm a parallel sequence trending NE-SW which is not folded or faulted, which is in keeping with the general trend of mapped units in the area. There is no outcrop in the region where these anomalies occur, so these anomalies provide extra information and constrain the geological interpretation of this area.

Modelling of the Brachina Formation reveals a lithomagnetic unit which strikes 010° and displays a steep easterly dip of 80°. This model fits the field data very well. The termination of the Brachina appears enigmatic from field mapping, as it is abruptly terminated by the Barrey's Tear Fault in the south. Possible explanations for the behaviour of the Brachina Formation at depth were postulated through information gained from aeromagnetic information.

Figure 5.1 Generalised structure and lithologies which have been mapped are shown and overlain by **Figure 5.1a** so that the geophysical constraints may be observed.

Figure 5.1 Figures 4.3 and 4.3a are used as an interpretation map so that real geophysical data and its interpretation may be compared with the mapped geology.

(Note that the geophysical data shown covers a larger area than the geological map area)

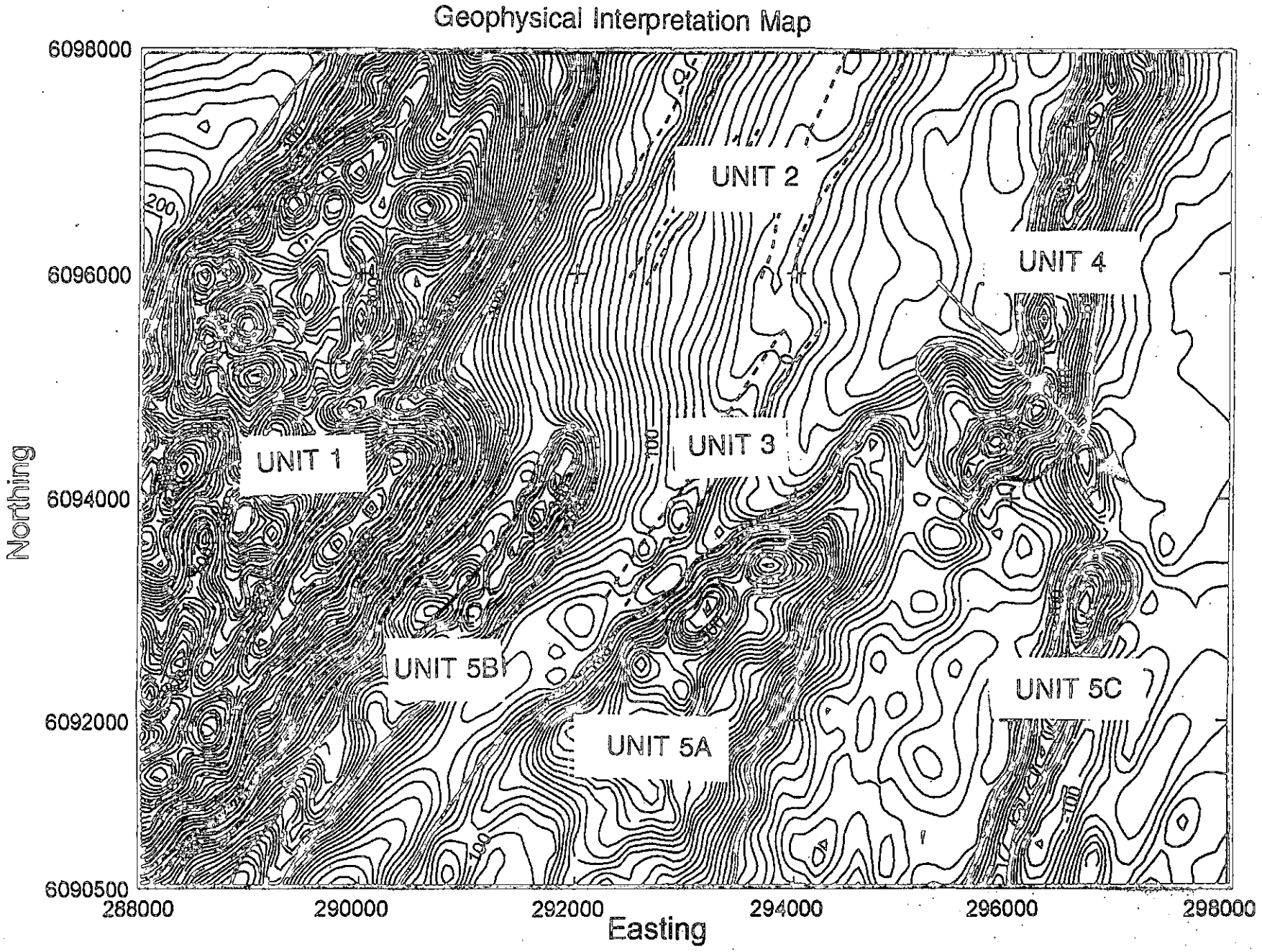
Geophysical Interpretation Map
6098000
6096000
6094000
6092000
6090500
Northing
288000
290000
292000
294000
296000
298000
Easting
UNIT 1
UNIT 2
UNIT 3
UNIT 4
UNIT 5A
UNIT 5B
UNIT 5C
200
300
100
100

Figure 5.1a

Geological Interpretation of Structural and Lithological boundaries at thesurface

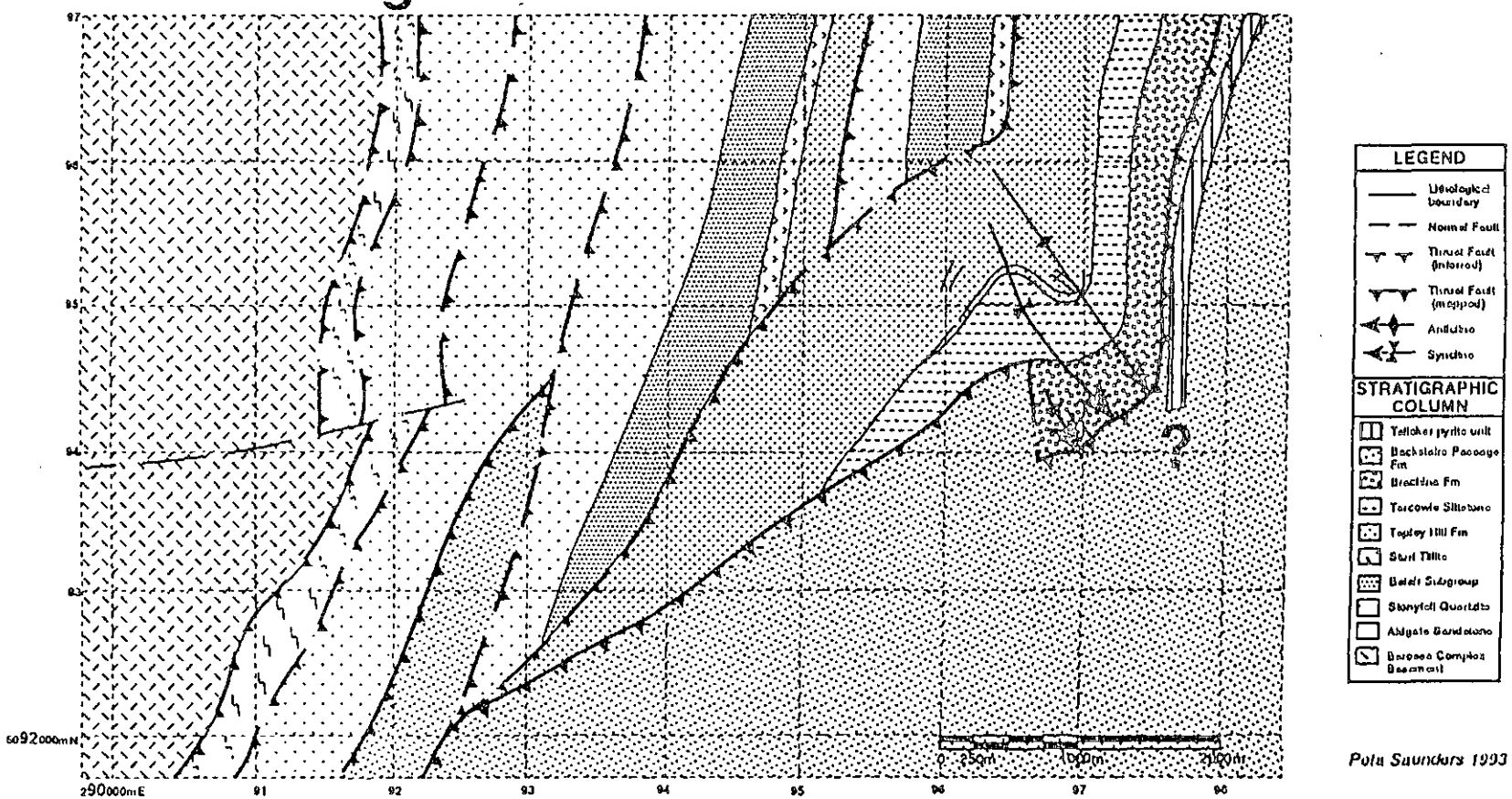

Figure 5.1

It is proposed that faulting of the Brachina Formation along the Barrey's Tear Fault has left the northern portion exposed and the southern portion remaining at depth beneath the Kanmantoo cover. Examination of lithomagnetic Unit 5A (Figure 4.3a) as defined by the TMI contour map (Figure 4.3) reveals steep contour intervals along the western margin (the BCT) and broader contour intervals along the eastern margin of this unit. The steeper contour intervals suggest a shallow sourced anomaly while the broader contour intervals suggest a magnetic body at a greater depth. Field studies reveal that outcropping rocks are of the Backstairs Passage Formation and yield high magnetic susceptibilities. This presents difficulties in distinguishing the signal of the overlying magnetic Backstairs Passage Formation, from the signal of underlying magnetic Brachina Formation. The broader source has been attributed to the signal received from the Brachina Formation at depth.

5.2 Cross Section Analysis

A deformed state cross section across the Still Range Imbricate Fan (Figure 3.4), was constructed and structures were considered viable (in the manner set out by Marshak and Woodward (1988)) for a foreland basin, tectonic province.

The deformed state cross section is dominated by a series of steep easterly dipping listric thrust faults of an imbricate fan. These thrusts have been propagated in an east to west manner. A major décollement exists within the basement and is responsible for bringing the basement to the surface as an anticlinal inlier as is seen in the western portion of the section. An upper basal detachment is situated between the basement and the Adelaidean contact which has resulted in the shearing of the Aldgate sandstone. Thrusting of the Adelaidean does not appear to involve the basement as shearing is suggested to have occurred along the rheological weakness that exists between the basement and the Adelaidean cover. Lithologies incorporated within thrust sheets exhibit minor curvature. However, the present level of erosion reveals their steepest dips. The eastern most area of the cross section reveals great displacement (the magnitude of which is unknown) along the reactivated BCT. The possibility of a duplex system is considered, as this may account for the same features as the suggested imbricate fan which are exhibited at this present erosional level.

5. 3 Evolution of structures

During the Delamerian orogeny change from an extensional to a compressional regime occurred. Maximum compressional stresses were oriented regionally in an East West direction (Jenkins, 1990). In the study area structural data comprising mineral and elongation lineations, fault and fold orientations suggest a tectonic transport direction from the E-SE to W-NW.

Jenkins (1986) proposed a tectonic model for the southern Adelaide Fold Belt, which involved the obduction of lithospheric crust to the east which caused sedimentary cover and basement abutting the Gawler craton to be subject to foreland basin deformation. This model suggests that thrust propagation occurs from east to west, implying the youngest faults occur to the west and the oldest to the east.

The sequence for the structural evolution of the Bull Creek area follows Jenkins (1990) model of east to west thrust propagation. The geometry of evolving structures in the Bull Creek area is greatly influenced by the positioning of the Adelaidean and Kanmantoo sediments prior to deformation (Figure 5.2a). This predeformation model suggests that Adelaidean sediments were deposited upon the basement in a manner which led to thinner deposition to the south east.

The Kanmantoo sediments of the Ashbourne wedge sequence were deposited as a thick sequence upon the Adelaidean (Figure 5.2a). This thickness may be explained by the thinning of Adelaidean deposits in the south which provided a depression for Kanmantoo Group sediment accumulation. Alternatively Adelaidean sediments below the Ashbourne wedge may have been eroded providing a channel which was filled with Kanmantoo Group channel deposit as suggested by Mancktelow (1979a). The Kanmantoo-Adelaidean boundary (now the BCT) is proposed to be a major syndepositional growth fault. This has formed during a cycle of lithospheric extension as suggested by Jenkins (1990). Sediment accumulation associated with growth faulting may have resulted in subsequent thickened deposition of the Kanmantoo Group above the down faulted block (which is east in this case). Evidence from aeromagnetic data suggests that the basement is at a much greater depth to the East of this fault, which supports the suggested large scale normal displacement along this fault. A combination of lateral thinning of the Adelaidean sediments, channel deposition and growth faulting can sufficiently explain the thickening of the Kanmantoo Group.

The first phase of compressional deformation (associated with the Delamerian orogeny) in the study area, induced the outcrop scale folding observed in the Backstairs Passage Formation sediments of the Ashbourne wedge. This may have accompanied thrust faulting within the Kanmantoo Group as Jenkins (1990) has suggested, although there is no field evidence in this study area to confirm the presence of thrust faults within the Kanmantoo Group. Reactivation of the BCT growth fault occurred next producing a steep listric fault with major (3-5km)

displacement along it, this fault possibly extends down to depths of about 7-10km before becoming horizontal.

The MCFTS is bound by the BCT and the SSCT. These are growth faults which have been reactivated during compression. This thrust sheet can be divided into northern and southern regions. In the northern zone, thrust sheet transportation is impeded by a block comprised of Adelaidean sediments (which are thicker here) and possibly a basement ramp.

The problem which the MCFTS presents is the juxtapositioning of younger Tapley Hill sediments which are shown to thrust up against older Stonyfell Quartzite (Figure 3.2: Map 1) and cross section (Figure 3.4). This is contrary to accepted thrust tectonic theories which suggest that older units are thrust up against younger units (Boyer and Elliot 1982). The proposed growth faulting in the area may solve this problem. Growth faulting leads to younger sediments being down faulted (Williams et al 1989), to the east in this case (Figure 5.2a). This would lead to older units such as the Stonyfell Quartzite being at a higher level than younger units such as the Tapley Hill Formation prior to the onset of thrusting.

The southern portion of the thrust sheet has been transported further west to northwest at a lower angle (Figure 5.2b). This is because there is no block in this area to impede thrust sheet transport. This is due to the thinned deposition of Adelaidean sediments in this area. The absence of a block in the south has resulted in a more south easterly transport direction. The faulting (Barrey's Tear Fault) and folding of the MCFTS within the Brachina Formation is the result of the difference in thrust transport direction of the northern and southern regions, but may also be a fault propagating a break thrust fold (the major anticline-syncline folds). The Barrey's Tear fault occurs perpendicular to the strike of bedding within the Brachina, this is a tear fault (after McClay 1992). This style of fault occurs when a thrust sheet progresses but is torn in half parallel to the movement direction of the propagating sheet. In this case tear faulting has resulted because of the difference between high angle thrusting in the north and the lower angle thrusting in the south (Figure 5.2b). This fault projects beneath the major folds of the area. The major anticline-syncline pair of the MCFTS may have developed as fault propagation folds. The tip line of the Barrey's Tear Fault projects beneath the MCFTS, where it is a blind fault which does not emerge at the surface at present erosional levels.

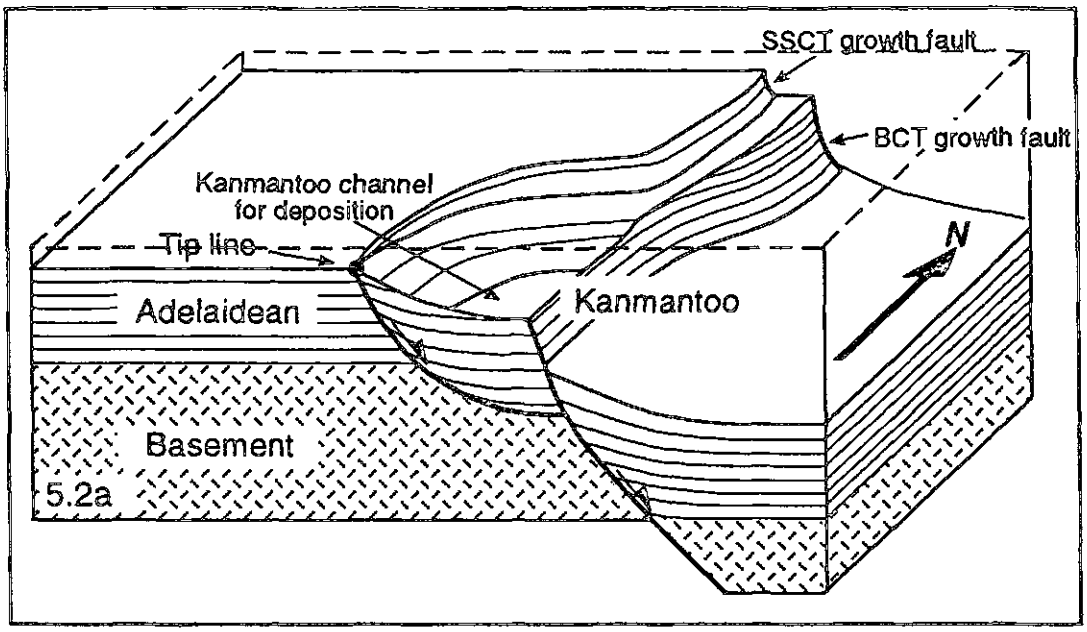

Figure 5.2a PRE- DELAMERIAN EXTENSIONAL REGIME. Growth faulting has occurred along the SSCT and BCT. The Tip line for the SSCT growth fault is observed in the south and is shown in the figure. Growth faulting has offset basement, Adelaidean and overlying Kanmantoo Group. Kanmantoo deposition may still have been occurring during this phase. The top of the Kanmantoo deposition is marked by the dashed line.

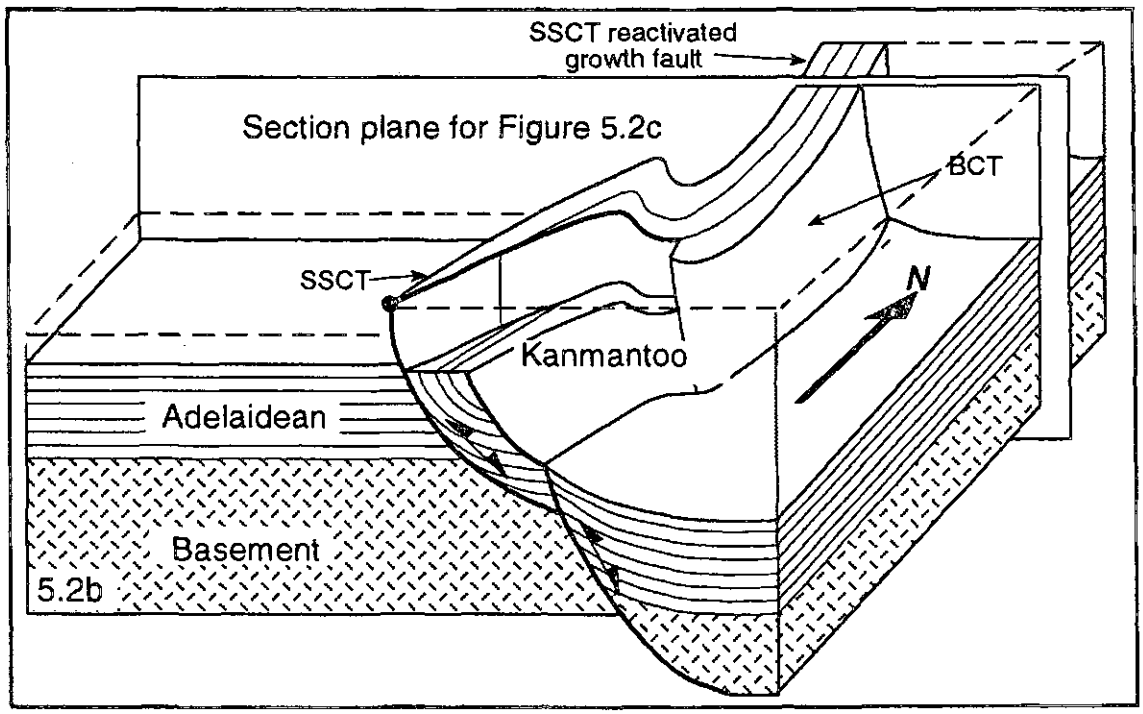

Figure 5.2b INITIAL PHASE OF DELAMERIAN DEFORMATION. The reactivation of the SSCT and the BCT occurs. The MCFTS is propagated during this phase and tear faulting of this thrust sheet occurs resulting in the southern portion of the thrust sheet being left at depth.

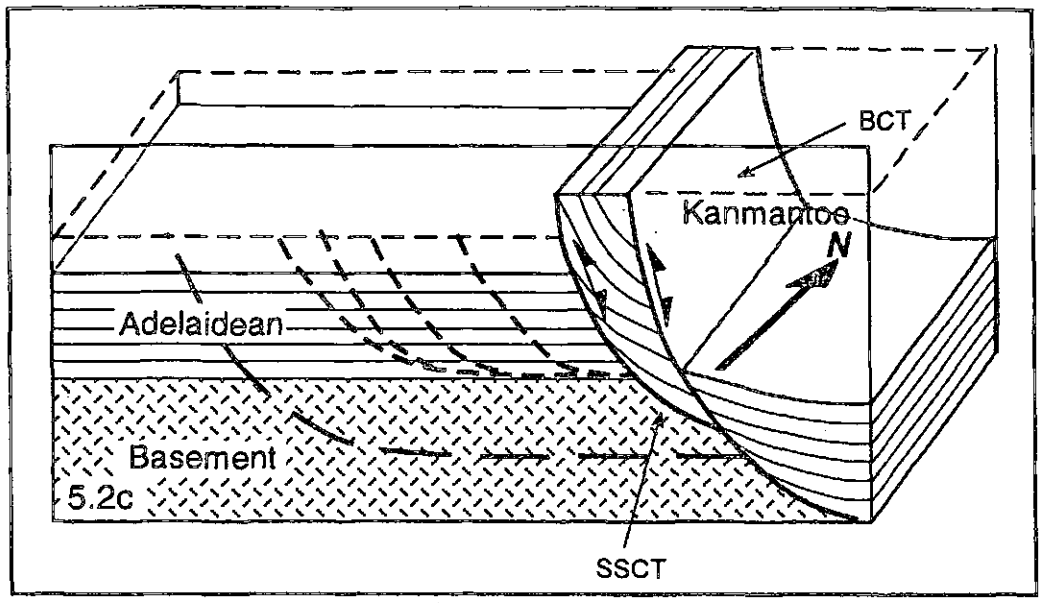

Figure 5.2c CONTINUED DELAMERIAN DEFORMATION (Section plate taken from Figure 5.2b) Heavy dashed lines show the path for imbricate thrust fault generation. The detachment (at the basement - Adelaidean contact) and basal décollement (within the basement) also appear as dashed lines. The Kanmantoo sediments still overly the Adelaidean sequence to the west and east of the BCT.

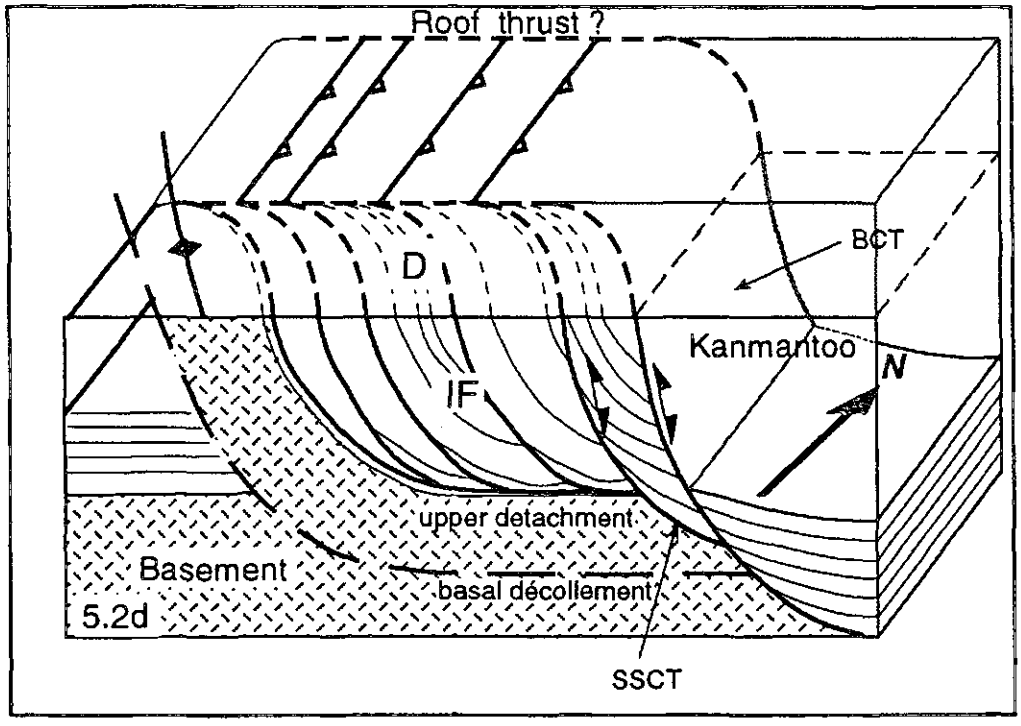

Figure 5.2d FINAL PHASE OF DEFORMATION (documented in this study) Imbricate stacking (or duplexing ?) occurs sequentially from east to west towards the foreland. Movement has occurred along the upper detachment. Finally the reactivation of the basal décollement has thrust a sliver of basement over the Adelaidean and possibly Kanmantoo sediments The present level of erosion is marked by the solid line and implies that either an imbricate fan or duplex system existed.

The Still Range Imbricate Fan (shown in Figure 3.4) was generated with subsequent compression which led to the shortening of the Adelaidean sequence as shown in the cross section . The Aldgate sandstone provides the interface for an upper detachment being a zone of weakness due to the contrasting rheological properties between rocks of the basement and cover sequence. Movement along the basement basal décollement may continue westwards at the same time but thrusting was transferred to the upper detachment during this phase resulting in Thrust sheets 1,2,3 and 4 being sequentially generated (Figure 5.2c). These thrust sheets are bound by high angle listric thrusts of an imbricate fan which have propagated up section from the upper detachment. These thrust sheets may be linked by a roof thrust in which case thrusts become sigmoidal faults of a duplex system (Figure 5.2d shows these as inferred thrusts) and thrust sheets are horses. The present erosional surface as shown in cross section has eroded the top half of the system obliterating any evidence which would suggest a roof thrust was present. For this reason the more common (according to Boyer and Elliott, (1982)) imbricate fan model was adopted. The Mt. Magnificent Re-entrant occurs as a result of thrust sheet amalgamation of Thrust sheet 2 and 3. Thrust sheet 2 has propagated over Kanmantoo Group sediments and incorporating them into the imbricate fan system.

The final phases of Delamerian deformation within this area have resulted in the activation of the basal décollement which transported a sheet (consisting of the upper 1-2km of the basement) westwards to form a haningwall anticline (McClay 1992) which lies upon a footwall comprised of basement (Figure 5.2d). During the transportation of the basement sheet the overlying cover sequence, comprising Adelaidean and Kanmantoo Group sediments are transported in a relatively undeformed state on top of this sheet (Figure 5.2d) although there is the possibility of further steepening of the SRIF. Some deformation may occur along the basement-Adelaidean contact, resulting from basement-cover dip slip shearing during the folding of the basement. The intensity of deformation on the eastern and western basement-cover contacts (Steinhardt, 1991) provides valuable evidence that thrusting within the basement, rather than regional scale folding alone (which would not produce such intense deformation) has brought basement up to the surface where it is exposed at the present level of erosion as an anticlinal inlier.

6. SUMMARY

6.1 Conclusions

Through integration of geophysical and structural data a model comprising a complex system of thrust faulting and associated thrust sheet generation has been established. An understanding of the pre-Delamerian distribution of stratigraphy is important. Growth faulting associated with basin extension has also affected the evolution of geological structures and has been taken into account. The comparison of magnetic susceptibilities at outcrops with aeromagnetic anomalies was important in discerning the difference between the Brachina Formation and the Kanmantoo magnetic cover. The Brachina Formation is postulated to lie at depth.

The difficulties associated with structural interpretation from limited outcrop have been eleviated by the application and interpretation of a high resolution aeromagnetic and radiometric survey. Prominent magnetic marker horizons, and their ready identification in outcrop (through susceptibility measurements) have contributed to the success of geological interpretation.

Stratigraphic repetition is explained by a model which suggests thrust faulting has occurred, bringing portions of the Adelaidean sequence to the surface as a repeated sequence. The thinning of the Adelaidean may be explained by depositional thinning, erosion of these sediments once deposited and also structural reasons (i.e. faulted at depth). The thickening of Kanmantoo Group sediments is sufficiently accounted for by deposition in a deep channel deposit and thickening attributed to sedimentation during growth faulting.

6.2 Recommendations

For an improved cross section, cross section restoration and an accurate estimate of shortening, strain values should be calculated. Further geophysical investigation may involve modelling of gravity data to reveal the depth to the basement. If drilling is undertaken in the region then stratigraphic units and the depth at which they are encountered should be compared with the cross section and structural interpretation at depth. Any drill holes intersecting lithomagnetic Unit 5C should be examined for magnetic mineral identification and oriented samples should be obtained for NRM measurements.

ACKNOWLEDGEMENTS

Thankyou to the many people who helped out with field work, especially Ray and Jean Stone of Nangkita and the "Barreys" who provided a roof over my head and some great meals after field work. SADME provided a great deal of logistical support and for that I thank them.

The support and encouragement from my supervisors Dr. Pat James and Dr. Shanti Rajagopalan, especially in the final stages was real BEAUT.

I would also like to thank my many "fieldies" for their rock spotting abilities and my friends the moo-moos !!!.

Many thanks are extended to all Ph.D students, in particular Scotty, Garry and Rob, for all their help, stress relief, support, encouragement.....(running out of adjectives), throughout the year!

The Shonky Geophysics boys (Shonky Bros. Inc. 1993) are thanked for accepting a pseudo geophycist into their ranks. Thanks to the other inmates of Cell Block 211a and other Honours students who have provided a much needed abundance of comic relief. I would also like to express gratitude to my "late night" chauffeurs (esp. Shonky Bros. Parking Services, $50, and my dear old dad).

Mum, Dad and the rest of my family are thanked for all their help with field work etc.. and just for reminding me of who I was and also for keeping clean clothes, food and a bed available for occasional times when I came home.

REFERENCES

Boyd, D. 1967. The contribution of airborne magnetic surveys to geological mapping, In: Morley, L.W. (ed.) Mining and Groundwater Geophysics, *Geological Survey of Canada, Economic Geology Report* **26**: 213-227.

Boyer, S.E. and Elliot, D. 1982. Thrust Systems. *Am. Assoc. Petrol. Geol. and Geophys.* **66** (9): 1196-1232.

Clarke G.L. and Powell R. 1989. Basement-cover interaction in the Adelaide Foldbelt, southern Adelaide Fold Belt. *Tectonophysics* **214.**

Fischer, M.P., Woodward, N.B.and Mitchell, M.M. 1992. The Kinematics of break thrust folds. *J.Struct. Geol.* **14** (4): 451-460.

Grant, F.S. 1985. Aeromagnetics, geology and ore environments, I. Magnetite in Igneous, Sedimentary and Metamorphic Rocks: An overview. *Geoexploration* **23**: 303-333.

Heaslip J.E. 1972. The Geology of the Mt. Magnificent area. B.Sc. (Hons)thesis, University of Adelaide (unpubl).

Jenkins, R.J.F. 1986. Ralph Tates enigma - and the regional significance of thrust faulting in the Mt. Lofty Ranges. *Geological Society of Australia, Abstracts.* **15:** 101

Jenkins, R.J.F. 1990. The Adelaide Fold Belt: Tectonic reappraisal. In: J.B.Jago and P.S. Moore (eds.) The Evolution of a late Precambrian - Early Palaeozoic Fift Complex : The Adelaide Geosyncline. *Geol. Soc. Aust. Spec. Publ.* **16**: 396-420.

Jenkins, R. and Sandiford, M., 1992, Observations on the tectonic evolution of the Southern Adelaide Fold Belt. *Tectonophysics* **214.**

Johnson, T.M. 1991. The structure of the Blowhole Creek area, southern Adelaide Fold Belt, Fleurieu Peninsula, South Australia. B.Sc. (Hons) thesis, University of Adelaide (unpubl)

Lister, G.S. and Snoke, A.W. 1984. S-C Mylonites. *J.Struct. Geology* **6** (6):617-638.

Mancktelow, N.S. 1979b. The Structure and metamorphism of the southern Adelaide FoldBelt: Ph.D. Thesis, University of Adelaide (umpubl)

Mancktelow, N.S. 1990. The structure of the southern Adelaide Fold belt, South Australia In: J.B. Jago and P.S. Moore (eds.) The evolution of a late Precambrian-Earlly Palaeozoic Rift Complex: The Adelaide Geosyncline. *Geol. Soc. Aust Spec. Publ.* 16:215-229.

Marshak, S. and Mitra, G. 1988. Basic Methods of Structural Geology. Prentice Hall Inc. 468 p.

McClay, K.R. 1992. Glossary of Thrust Tectonic Terms. In: Thrust Tectonics. Chapman and Hall 447 p.

Menpes, R.J. 1992. Structural Evolution of a Transpression zone in the southern Adelaide Fold Belt: Northeast Dudley Peninsula, Kangaroo Island. B.Sc (Hons) Thesis, University of Adelaide (unpubl)

Nelson J.B., 1988. Comparison of gradient analysis techniques for linear two-dimensional magnetic sources. *Geophysics* **7** (8): 1088-1095.

Offler,R. and Fleming, P.D. 1968. A synthesis of folding and metamorphism in the Mt. Lofty Ranges, South Australia. *J. Geol. Soc. Aust.* **15** (2): 245-266.

Parkin, 1969. Handbook of South Australian Geology. Ed. L.W. Parkin. Geol. Survey of South Australia 268p.

Passchier, C.W. and Simpson,C. 1986. Porphyroclast systems as kinematic indicators. J. Struct. Geol. 8(8): 831-843.

Preiss, W.V. (Compiler) 1987. The Adelaide Geosyncline- late Proterozoic stratigraphy, sedimentation, palaeontology and tectonics. Geol.Surv.S. Aust., Bulletin 53, 438pp

Ramsay, J.G. 1967. Folding and fracturing of rocks. McGraw Hill, New York, 567pp.

Rogers, J.R. 1991. The structure of the Talisker area, southern Adelaide Fold Belt, Fleurieu Peninsula, South Australia. University of Adelaide B.Sc. (Hons.) thesis, (unpubl)

Rajagopalan, S. 1989. Aeromagnetic interpretation of the Kanmantoo Group South Australia. Ph.D. thesis, University of Adelaide (unpubl)

Rajagopalan, S. and Boyd, D.M., 1989. A systematic approach to displaying aeromagnetic data. *J.Assoc. Expl. Geophys.* **10** (1): 19-29.

Rumble, D. 1973. Fe-Ti Oxide Minerals from Regionally Metamorphosed Quartzites of Western New Hampshire. *Contr. Mineral. and Petrol.* **42**: 181-195.

Sibson, R.H. 1977. Fault Rocks and fault Mechanisms. *J. Geol.Soc. London* **133**:191-213.

Steinhardt, C. 1991. The microstructural anatomy of a major thrust zone on Fleurieu Peninsula, South Australia. *Aust. J. Earth Science*. **38**: 139-150.

Telford, W.M.,Geldart, L.P. and Sheriff, R.E. 1990. Applied Geophysics. Cambridge University Press.

Valenta, R.K., Jessell, M.W., Jung, G. and Bartlett, J. 1992. Geophysical interpretation and modelling of threee dimensional structure in the Duchess area, Mount Isa, *Aust. Expl. Geophys*. **23**: 393-400.

Whiting, T.H. 1986. Aeromagnetics as an aid to geological mapping - a case history from the Arunta Inlier, Northern Territory. *Aust. J. Earth. Science* **33**: 271-286.

Wise, D.U., Dunn, D.E., Engelder, J.T., Geiser, P.A., Hatcher, R.D., Kish, S.A., Odom, A.L., Schamel, S. 1984. Fault-related rocks: Suggestions for terminology. *Geology* **12** :391-394.

Wymond, A.P. 1950. The Geology of the Bull Creek Area. (M.Sc.) thesis. University of Adelaide (unpubl).

APPENDIX 1

Thin Section Localities

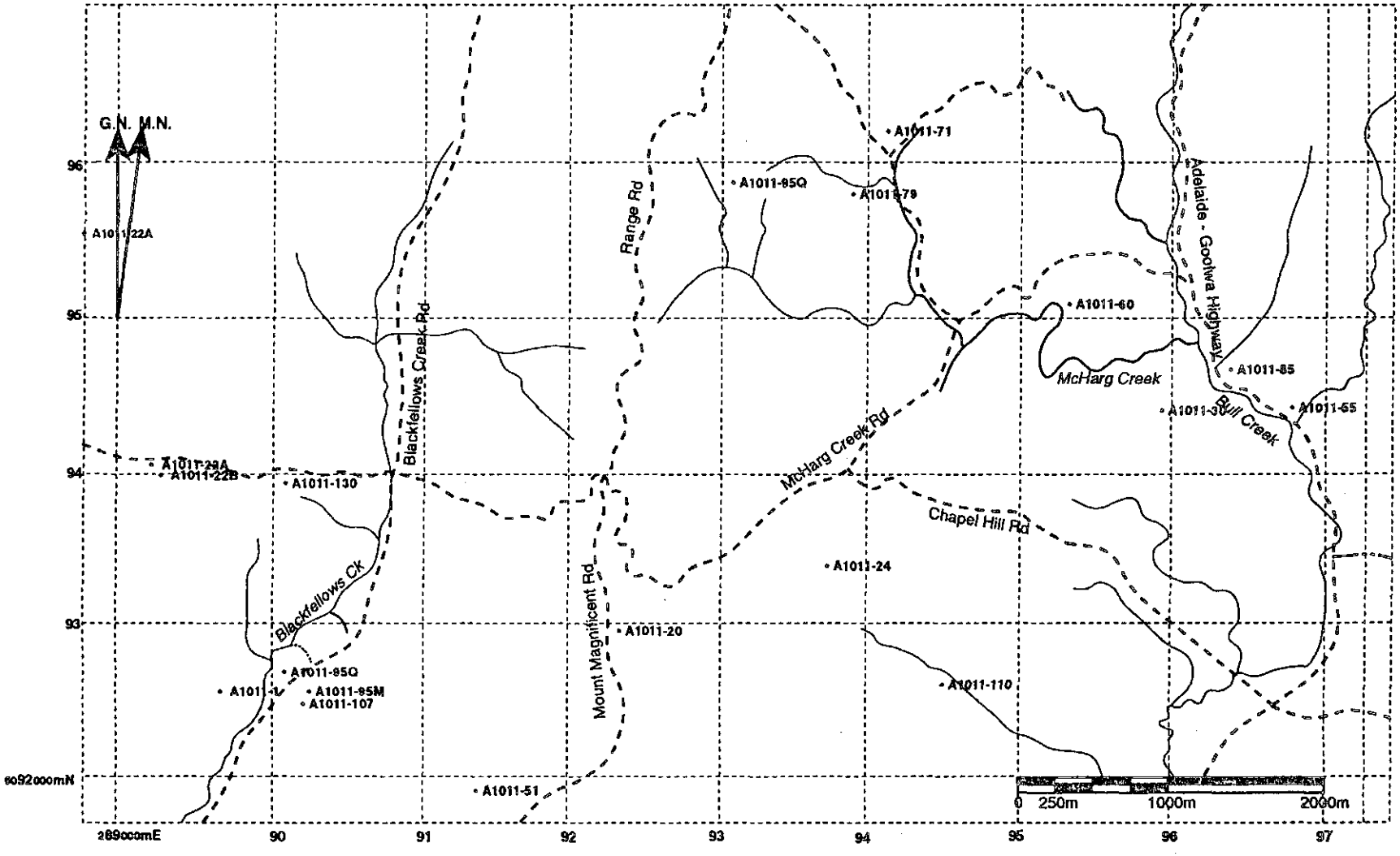

APPENDIX 1

TS denotes Thin Section
PTS denotes Polished Thin Section
All of the following samples are accompanied by Hand Samples and are lodged with The University of Adelaide, Department of Geology and Geophysics.

SAMPLE	STRAT. FM.	MINERALS	DESCRIPTION
TS A1011 - 1	Barossa Complex	45% Quartz 40% Garnet 6% Sericite 5% Biotite 5% Muscovite	The rock is gneissic and is dominated by quartz augens which show undulose extinction and subgrain formation. Retrogressed garnet porphyroblasts are abundant. Biotite, muscovite and sericite define the schistosity.
TS A1011 - 22A	Barossa Complex	80% Quartz 10% Sericite 4% Biotite 0.5% Pyrite 0.5% Chlorite >1% Magnetite	Quartz is present as elongate augen shaped grains, with micaceous minerals wrapping around grains , defining the dominant schistosity. Magnetite occurs as needlelike grains which are aligned parallel to the dominant schistosity.
PTS A1011 - 22B	Barossa Complex	45% Quartz 20% Muscovite 20% Biotite 10% Sericite <1% Magnetite	Quartz appears blue and displays subgrain formation indicating its subjection to high strain. Elongate recrystallised quartz grains are surrounded by micaceous minerals which define the dominant schistosity. Magnetite occurs as needlelike grains aligned parallel to the dominant schistosity.

PTS A1011 - 130	Barossa Complex	30% Sericite 30% Quartz 20% Biotite 15% Muscovite 2-3 % H/Blende 2-3% Magnetite	Banded schist/gneiss (2-5mm bands) alternating between mica rich layers and quartz rich layers. Quartz shows undulose extinction and some subgrain formation indicating it is highly strained. Sericite, biotite and muscovite define the main schistosity. Magnetite occurs as needlelike grains aligned parallel to the main schistosity.
TS A1011-93B XZ&YZ	Aldgate Sandstone	50% Quartz 40% Plagioclase 5% Microcline 2-5%Sericite <1% Ilmenite	Ultramylonite displaying quartz ribbons which exhibit undulose extinction and display recrystallisation. Feldspars occur between quartz ribbons (which form bands) and have been recrystallised. Sericite occurs as the result of retrogressive metamorphism of feldspars.
TS A1011- 51	Backstairs Passage Fm	50% Quartz 30% Plagioclase 15% Microcline 5% Sericite	Homogeneous fine grained sandstone. Quartz shows distinct subgrain formation within larger grains. Grain boundaries are sutured. Some felsdpars have been replaced during retrograde metamorphism by sericite.
TS A1011-107	Aldgate Sandstone	40% Microcline 35% Quartz 15% Plagioclase 10% Sericite <1% Ilmenite	Mylonite characterised by asymmetric feldspar porphyroclasts and quartz ribbons.
TS A1011 - 95M XZ	Aldgate Sandstone	50% Quartz 35% Microcline 8% Sericite 5% Plagioclase 5% opaques 2% Muscovite <1% Chlorite	Quartz/Feldspar mylonite showing recrystallisation. Layering consists of quartz ribbons and recrystallised feldspars occuring between these ribbons. Mylonitic foliation is defined by ilmenite and micaceous minerals and orientation of quartz ribbons.

TS A1011 - 20	Stonyfell Quartzite	99% Quartz <1% opaques	Massive white quartzite shows dynamic recrystallisation which has led to quartz subgrain formation and a dominant flattening direction, indicating inhomogeneous high strain.
TS A1011 - 95Q XZ	Stonyfell Quartzite	90% Quartz 10% Plagioclase <1% Opaques	Quartz grains show undulose extinction. Fine grain subgrains form at grain boundaries of larger quartz grains. Quartz and plagioclase define elongation lineations observed in hand specimen.
TS A1011 - 79 XZ & YZ	Sturt Tillite	**Clasts 30%** 75% Quartz 20% Carbonates 5% Gneissic **Matrix 70%** 70% Fine grain indistinguishable clay minerals 30% Biotite and Chlorite	Elongate clasts are aligned parallel to the cleavage. Quartz clasts display undulose extinction and subgrain formation within them. Pull apart clasts are observed (indicating high strain). Platey clay minerals define the cleavage which wraps around clasts.
TS A1011 - 71 XZ & YZ	Tapley Hill Fm	70% Quartz 20% Biotite 10% Chlorite and muscovite	Bedding is defined by alternation of white (coarse grained) and blue-grey (fine grained) layers. Quartz is present as elongate quartz porphyroclasts (which are highly strained) with micaceous minerals describing the cleavage which is at 40° to bedding.
TS A1011 - 24	Backstairs Passage Fm	60% Quartz 40% f.gr. micas & clays	Sample from fault zone. No particular layering is observed. Biotite and muscovite show no preferred orientation.

TS A1011 - 90	Tapley Hill Fm	60% Quartz 35% Biotite <5% Chlorite <2% Opaques	Banding consists of psammitic and pellitic layering. Quartz grains are fine grained and do not show any flattenning. Micaceous minerals display little preferred orientation. Pellitic layers show slightly more orientation and higher strain than psammitic units. However strain is relatively low overall.
PTS A1011 - 60	Brighton Limestone	90% Calcite 8% Quartz <2% opaques	Calcite grains show reflection form cleavage surfaces and are extremely flattened and rock is almost totally recrystallised. Opaques are scattered throughout randomly and quartz grains show recrystallisation.
PTS A1011 - 30	Brachina Formation	65% Quartz 30% Biotite and fine grain micas <5% Magnetite	Steel grey siltstone. Banding is defined by heavy mineral layering. Conjugate kink folds are observed. The micaceous minerals define cleavage which appears parallel to bedding. Euhedral magnetite grains show only slight weathering (martitisation of mt to ht is weak)
PTS A1011 - 85	Brachina Formation	as above	as above This sample shows a cm scale break thrust fold.
TS A1011 - 55	Talisker	30% Pyrite 35% Quartz 35% Micas <1% chalcopyrite	Pyritic shale. Pyrite occurs as discrete discontinuous bands (pyrite lenses). These rocks are composed of 30µm bands. Micas define a fabric between these bands.